JUL 25 2000

SANDIA REPORT

SAND2000-1408
Unlimited Release
Printed July 2000

Evaluation of the $Li(Si)/FeS_2$ and $Li(Si)/CoS_2$ Couples for a High-Voltage, High-Power Thermal Battery

Ronald A. Guidotti and Frederick W. Reinhardt

Prepared by
Sandia National Laboratories
Albuquerque, New Mexico 87185 and Livermore, California 94550

Sandia is a multiprogram laboratory operated by Sandia Corporation, a Lockheed Martin Company, for the United States Department of Energy under Contract DE-AC04-94AL85000.

Sandia National Laboratories

Issued by Sandia National Laboratories, operated for the United States Department of Energy by Sandia Corporation.

Printed in the United States of America. This report has been reproduced directly from the best available copy.

Available to DOE and DOE contractors from
U.S. Department of Energy
Office of Scientific and Technical Information
P.O. Box 62
Oak Ridge, TN 37831

Telephone: (865)576-8401
Facsimile: (865)576-5728
E-Mail: reports@adonis.osti.gov
Online ordering: http://www.doe.gov/bridge

Available to the public from
U.S. Department of Commerce
National Technical Information Service
5285 Port Royal Rd
Springfield, VA 22161

Telephone: (800)553-6847
Facsimile: (703)605-6900
E-Mail: orders@ntis.fedworld.gov
Online order: http://www.ntis.gov/ordering.htm

DISCLAIMER

Portions of this document may be illegible in electronic image products. Images are produced from the best available original document.

SAND2000-1408
Unlimited Release
Printed July 2000

Evaluation of the Li(Si)/FeS_2 and Li(Si)/CoS_2 Couples for a High-Voltage, High-Power Thermal Battery

Ronald A. Guidotti and Frederick W. Reinhardt
Power Sources Engineering and Development Department
Sandia National Laboratories
P.O. Box 5800
Albuquerque, NM 87185-0614

Abstract

A detailed evaluation of the Li(Si)/FeS_2 and Li(Si)/CoS_2 couples was undertaken to determine which was better suited for use in a thermal battery with challenging high-voltage and high-power requirements. The battery was to produce a minimum voltage of 205 V during pulses of 36 A superimposed on a 6-A background load. The final design called for two 96-cell batteries in series, with each providing 1.1 kW background load, with peak power levels of 6.7 kW. The battery lifetime was to be 5 min. Since it was not possible to duplicate the desired complex waveform exactly, an alternate approximating constant-current load profile was used.

Single-cell tests were carried out at temperatures of 400°C – 550°C using the standard LiCl-KCl eutectic, the low-melting LiBr-KBr-LiF eutectic, and the all-lithium LiCl-LiBr-LiF minimum-melting electrolyte. These screening studies were then extended to 10-cell and 25-cell batteries at the same equivalent load conditions. Both 1.25"-dia. and 2.25"-dia. stacks were tested. Based on these tests, the best overall results were obtained using the all-Li electrolyte with the CoS_2 cathode and flooded anodes. The next best electrolyte was the low-melting electrolyte. A preliminary test with a 95-cell battery showed better performance than what was expected based on results of 10- and 25-cell tests, due to lower cell resistance.

Acknowledgments

The authors wish to acknowledge the assistance of Jim Gilbert, 2523, and Arlen Baldwin, formerly of 2523, who were the design engineers of the final battery.

Larry Moya and Frank Lasky, 2522, constructed and tested the 10-cell and 25-cell batteries.

Contents

Figures

Tables

Evaluation of the $Li(Si)/FeS_2$ and $Li(Si)/CoS_2$ Couples for a High-Voltage, High-Power Thermal Battery

INTRODUCTION

The battery-development department at Sandia National Laboratories was asked to develop a battery for an application that required both high power as well as high voltage. The performance requirements were: a lifetime of five minutes, a peak voltage of 360 V and a minimum voltage during pulsing of 205 V. The background current of 6 A is increased to 36 A during pulsing. It was felt that a high-power, high-voltage (HPHV) thermal battery was the most appropriate choice for this application. The preliminary battery design that was considered incorporated two series stacks of 96 cells each with a diameter of 2.25 inches. A 96-cell battery using the $Li(Si)/FeS_2$ technology, for example, would develop 96*1.94 V or 186.2 V open circuit. The load profile that was developed for testing was based on constant current and approximated the true load profile, which was quite complex. The background load of 6 A corresponded to a steady-state power of 1.1 kW and the 36-A load during pulsing corresponded to 6.7 kW.

We approached our mission with the objective of first identifying the appropriate electrochemical system and electrolyte, since what works well for one application may not function as desired for another. This was accomplished through a series of single-cell screening tests using two potential cathodes: FeS_2 and CoS_2. Three electrolytes were chosen for evaluation: the standard LiCl-KC1 eutectic (melting point=352°C), the so-called "low melting" LiBr-KBr-LiF eutectic (melting point=324.5°C),[1] and the all-Li LiCl-LiBr-LiF minimum-melting electrolyte (melting point=436°C). The screening tests were performed with 1.25"-dia. cells. We then tested the best combinations in 10- and 25-cell batteries using both 1.25"-dia. and 2.25"-dia. pellets, with the loads adjusted to the same current density in both cases. The final objective was to test the prime candidate system in a 96-cell battery. This report documents the results of the study.

EXPERIMENTAL PROCEDURE

Materials

The materials used for the initial screening studies are listed in Table 1. All separator mixes used Merck (now Calgon) Maglite 'S' MgO.

Testers

Single-Cell Tests – A HP6060B 60-A/300-W programmable electronic load was used for the initial single-cell screening tests. Two HP3458A high-speed DVMs were incorporated—one for the cell/battery voltage and the other for the current—to allow digitization of the pulses applied during discharge. A schematic of the test setup is shown in Figure 1. Considerable time was spent developing the necessary software to allow testing of the single cells under a wide range of discharge profiles. The need of critical timing and triggering of the load and DVMs, to capture

Table 1. Materials used for Single-Cell Screening Studies*

Anode: 44% Li/56% Si, with no added electrolyte (unflooded)
45% Li/56% Si, with 25% free electrolyte (flooded) (75% active material)
Cathodes: 73.5% FeS_2/25% separator/1.5% Li_20 (fused, lithiated)
73.5% CoS_2/25% separator/1.5% Li_20 (fused)
Separators: Standard (melting point = 352°C): 65% LiCl-KC1/35% MgO
Low-melting (melting point = 324.5°C): 75% LiBr-KBr-LiF/25% MgO
All-Li (melting point = 436°C): 65% LiCl-LiBr-LiF/35% MgO

* All values are reported in weight percent.

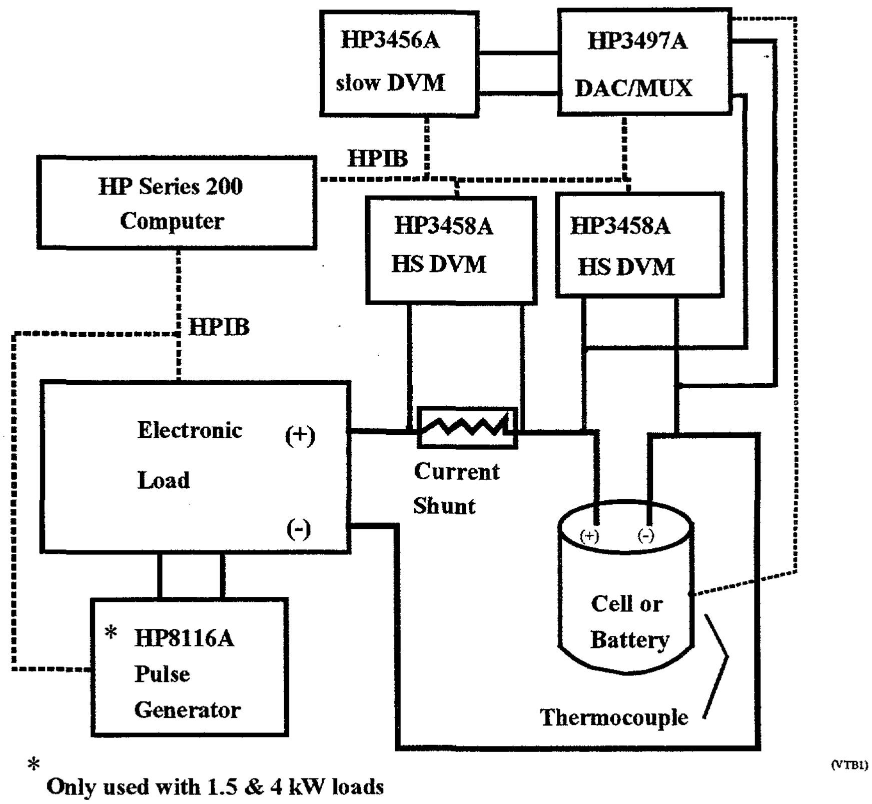

Figure 1. Experimental Test Setup Used to Test Single Cells and Batteries.

the entire response during pulsing, posed challenges.

The actual load profile that was to be used for the HVHP battery was beyond the capability of the HP6060B electronic load. Consequently, it was necessary to develop a modified load profile, which is shown in Figure 2. The duty cycles were changed to reflect the capabilities of the different electronic loads.

Battery Tests – For the initial 10-cell tests, it was possible to use the HP6060B 300-W electronic load with the same software used for single-cell tests. However, this load could not deliver enough power for testing of 25-cell batteries. In its place, we used a Transistor Devices 1.5-kW electronic load with a voltage rating of 150 V. The load profile of the 1.5-kW electronic load could not be programmed internally as was the case with the HP6060B electronic load. Consequently, it was necessary to program the load through its remote input with a HP8116A programmable function (pulse) generator. By programming the offset, width, and amplitude of the pulse, it was possible to obtain the required load profile. Interfacing the electronic load with the pulse generator required modification of the test-program software. Once this was done, the load performed quite well in the testing of 25-cell batteries.

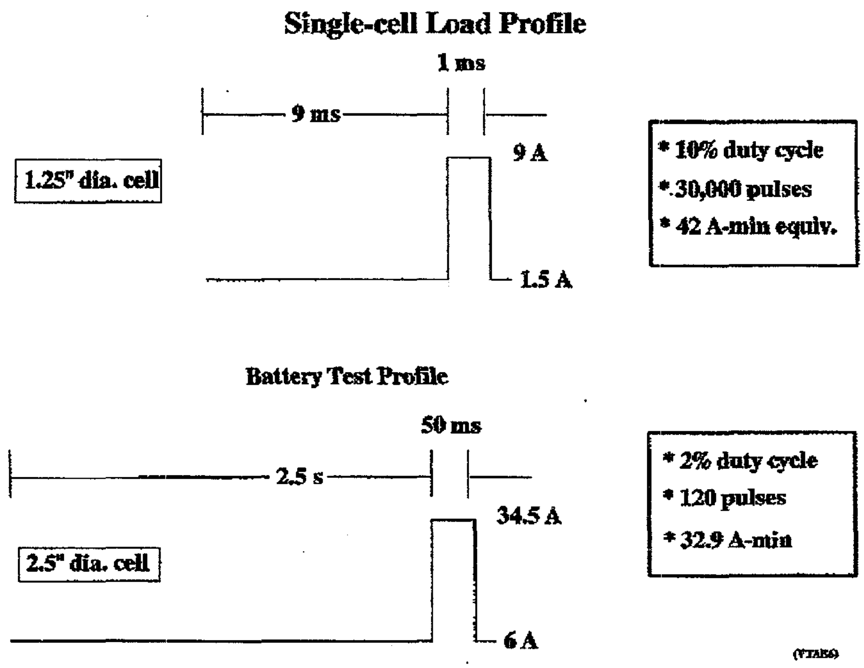

Figure 2. Actual Load Profiles Used for Testing Cells and Batteries.

The load requirements for testing of a 96-cell battery greatly exceeded that of the 1.5 kW electronic load. For these tests, it was necessary to use an electronic load bank made up of two Transistor Devices 4 kW modules in parallel, each rated at 400 V. We were able to use the pulse generator to program the 4 kW modules to the same load profile as for the 1.5-kW units.

Single-cell Screening Studies

Test Conditions – The test conditions used for the single-cell screening studies are summarized in Table 2. These current densities are the same as those for a full-sized battery based on a stack diameter of 2.5 inches. The temperatures that were chosen bracket those typical for a normally functioning thermal battery. The optimum separator or electrolyte-binder (EB) compositions had been previously determined for each electrolyte.

The cells were subjected to the load profile continuously during the entire discharge. However, to minimize data-storage requirements and to reduce the time necessary for data transfer from the

Table 2. Conditions Used for Single-Cell Screening Studies.

Cell diameter: 1.25"
Temperatures: 400°, 450°, 500°, 550°C
Duty cycle: 10% (9 ms steady state/1 ms pulse)
Currents: 1.5 A steady state/9 A pulse
Current densities: 190 mA/cm^2 steady state/1,140 mA/cm^2 pulse

DVMs to the controller, the cells were not sampled continuously. Instead, data were taken at 5 s, 60 s, 120 s, 180 s, 240 s, and 300 s for a time of 700 ms for each burst of readings.

RESULTS AND DISCUSSION

Single-Cell Tests

Electrolyte Effects - A typical cell response under the test load is shown in Figure 3 for a Li(Si)/FeS_2 cell based on the all-Li system. The upper trace is the current through the cell and the bottom is the response of the cell voltage.

The parameters that were examined for evaluation purposes were:

- Maximum time for sustaining the programmed pulse current
- Minimum cell voltage during the pulse
- Voltage loss during the pulse
- Total cell polarization (internal resistance)

The first two parameters should be as large as possible, while the latter two should be as small as possible.

The effects of electrolyte on the sustained pulse current for tests conducted at 450°C are summarized in Figures 4 and 5 for Li(Si)/FeS_2 and Li(Si)/CoS_2 cells, respectively, for unflooded anodes. For the FeS_2 cells (Figure 4), the pulse current could be sustained for the longest time with the all-Li electrolyte, since it does not show the polarization losses associated with the other two multi-cation electrolytes. The low-melting electrolyte could sustain the pulse current longer than the standard electrolyte. These trends were also evident at the higher temperatures.

For the CoS_2 cells (Figure 5), the electrolyte differences were not evident. All cells were able to maintain a current of 9 A for 180 s before dropping because of loss in anode capacity. The relative differences in performance of CoS_2 and FeS_2 are related to differences in discharge mechanism. For FeS_2, the first discharge step is:

$$FeS_2 + 3/2\ Li^+ + 3/2\ e^- \longrightarrow 1/2\ Li_3Fe_2S_4 \qquad [1]$$

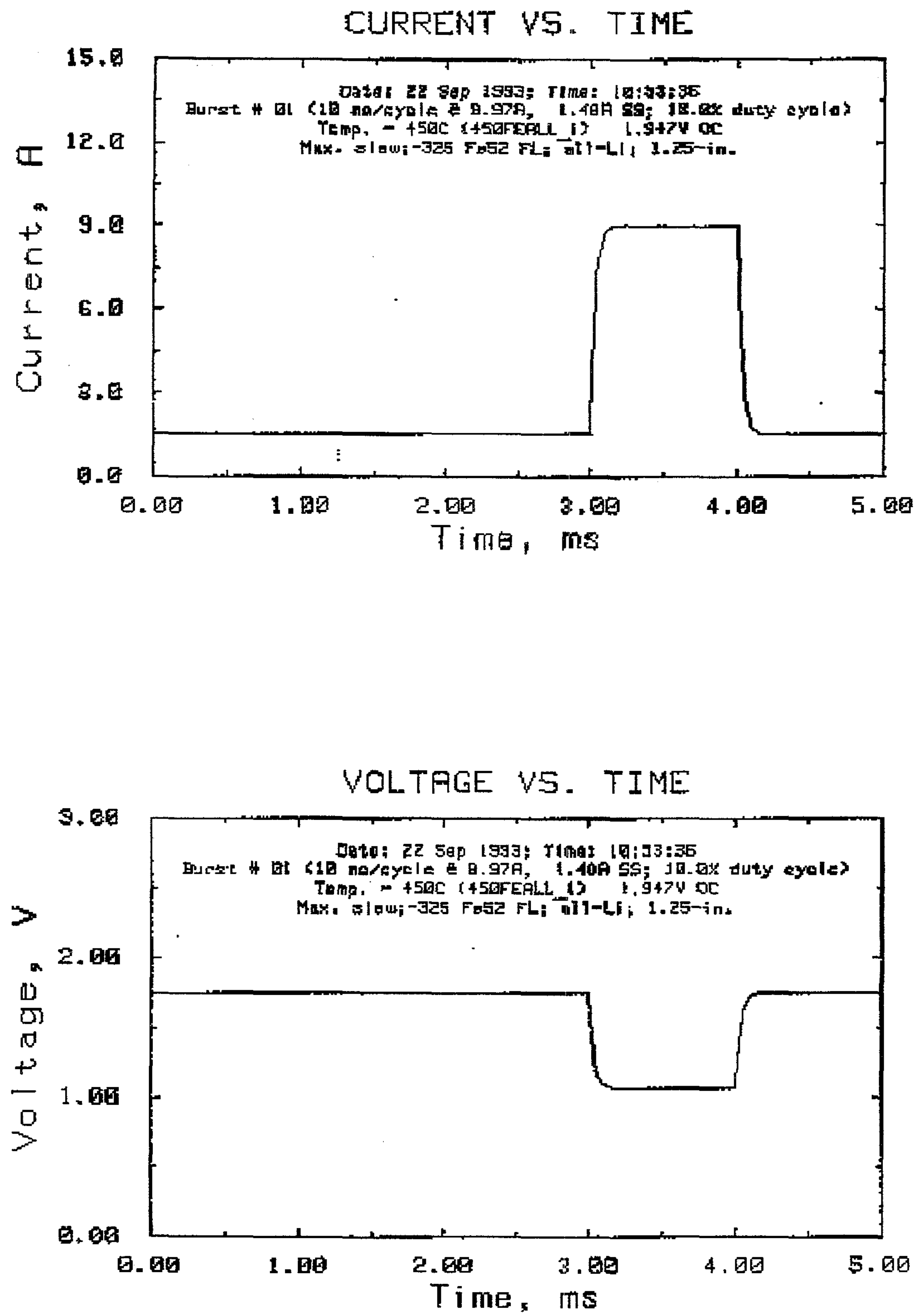

Figure 3. Current and Voltage Response of a Li(Si)/LiCl-LiBr-LiF/FeS_2 Single Cell Tested at 450°C at 1.5-A Background Load and 9.0-A Pulse Load (10% Duty Cycle; 1-ms Pulse Time).

The $Li_3Fe_2S_4$ is further reduced to Li_2FeS_2 according to eqn. 2:

$$Li_3Fe_2S_4 + Li^+ + e^- \longrightarrow 2\ Li_2FeS_2$$

[2]

For CoS_2, the first discharge step is:

$$CoS_2 + 4/3\ e^- \longrightarrow 1/3\ Co_3S_4 + 2/3\ S^{-2} \quad [3]$$

This material can be further discharged according to eqn. 4:

$$Co_3S_4 + 8/3\ e^- \longrightarrow 1/3\ Co_9S_8 + 4/3\ S^{-2}$$

[4]

The effects of electrolyte on the minimum pulse voltage for tests conducted at 450°C are summarized in Figures 6 and 7 for Li(Si)/FeS_2 and Li(Si)/CoS_2 cells, respectively, for unflooded anodes. For the FeS_2 cells (Figure 6), the largest minimum pulse voltage was shown by the all-Li cells; the minimum pulse voltages for low-melting cells were slightly greater than those for the standard cells for only the initial portion of discharge. The same trends were evident for the CoS_2 cells (Figure 7). Similar results were observed at the higher temperatures.

The effects of electrolyte on the voltage losses during pulsing for tests conducted at 450°C are summarized in Figures 8 and 9 for Li(Si)/FeS_2 and Li(Si)/CoS_2 cells, respectively, for unflooded anodes. For the FeS_2 cells (Figure 8), the lowest voltage losses by far were exhibited by the all-Li

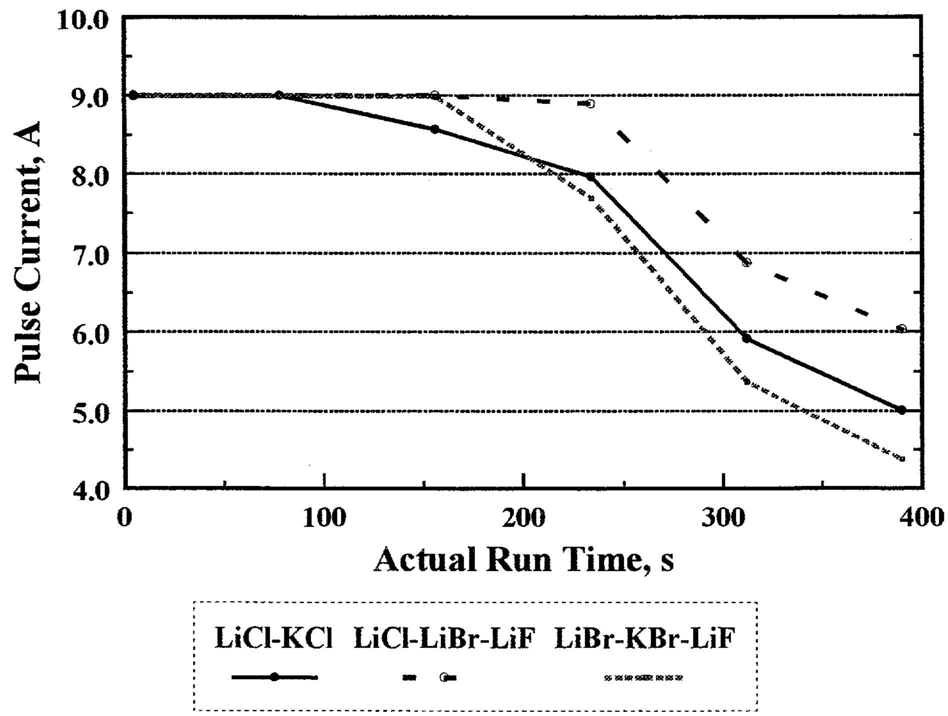

Figure 4. Pulse Current for Single Cells Tested at 450°C for Various Electrolytes for FeS_2-Based Catholyte .

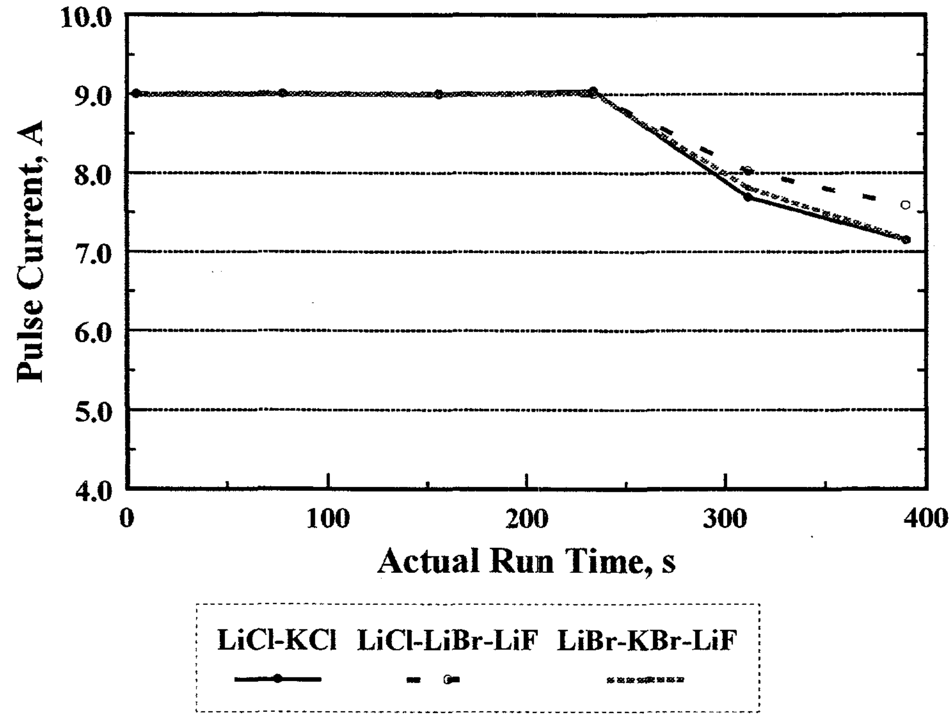

Figure 5. Pulse Current for Single Cells Tested at 450°C for Various Electrolytes for CoS_2-Based Catholyte.

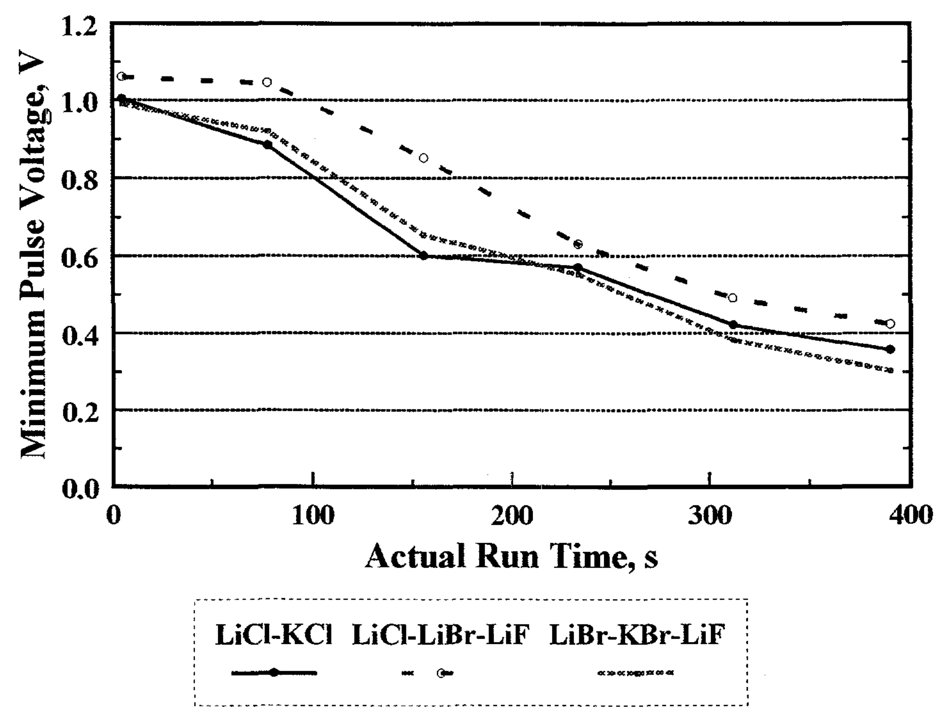

Figure 6. Minimum Pulse Voltage for Single Cells Tested at 450°C for Various Electrolytes for FeS_2-Based Catholyte.

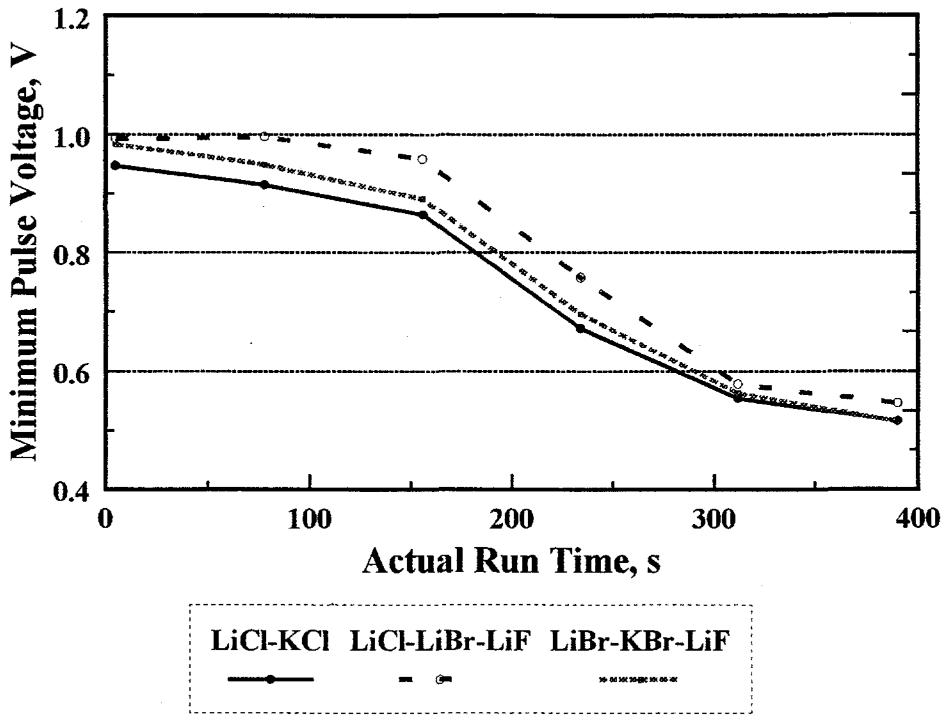

Figure 7. Minimum Pulse Voltage for Single Cells Tested at 450°C for Various Electrolytes for CoS_2-Based Catholyte.

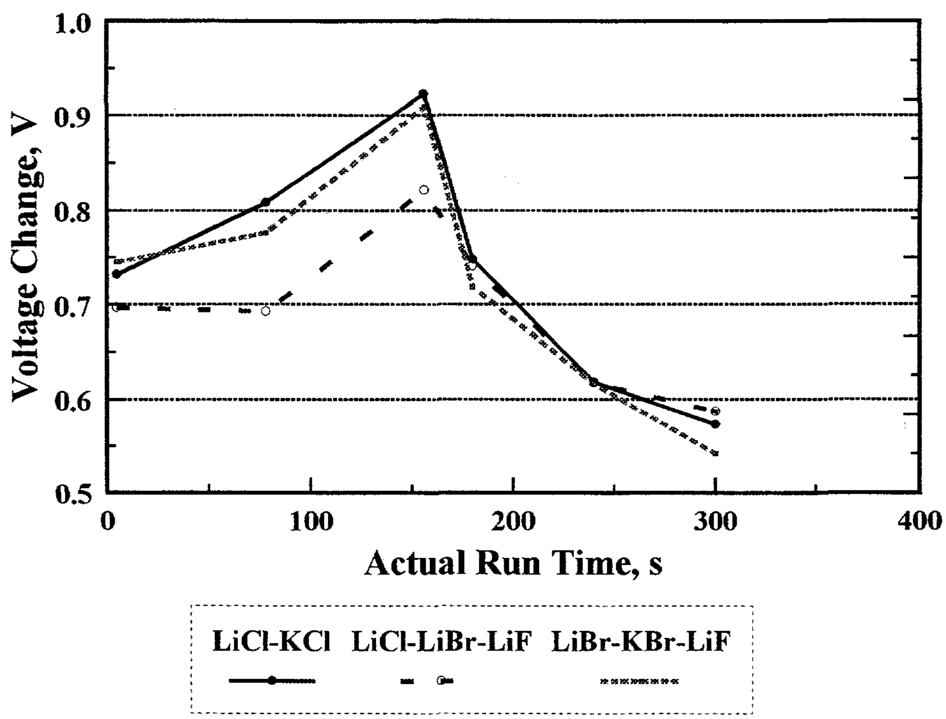

Figure 8. Voltage Change During Pulse for Single Cells Tested at 450°C for Various Electrolytes for FeS_2-Based Catholyte.

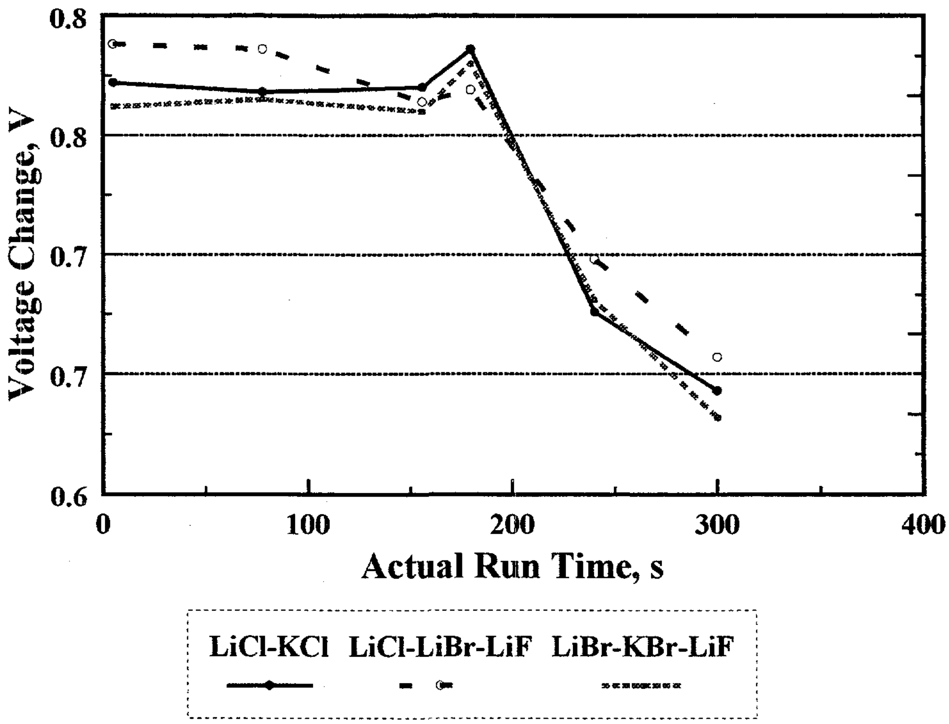

Figure 9. Voltage Change During Pulse for Single Cells Tested at 450°C for Various Electrolytes for CoS_2-Based Catholyte.

cells, followed by the low-melting cells. The loss in voltage showed a maximum with depth of discharge or run time. This reflects the nature of the first discharge phase, $Li_3Fe_2S_4$. For the CoS_2 cells (Figure 9), the relative differences among the electrolytes were not as great as for the FeS_2 cells (Figure 8) and the curve shape was different because of the nature of the discharge mechanism for CoS_2.

Based on the current and voltage changes during the pulses, an effective cell resistance or total polarization can be calculated using the formula of eqn. 5:

$$\eta_{total} = R_{cell} = (\text{delta } V_{pulse})/(\text{delta } I_{pulse}) \qquad [5]$$

(This resistance includes both ohmic and concentration/migration contributions. For a purely ohmic resistance, the cell voltage response exhibits a clean square wave during a pulse. However, with increased contributions of concentration polarization and migration effects, increased rounding of the corners occurs.)

The effects of electrolyte on the total polarization calculated using this equation are shown at 450°C in Figure 10 and 11 for Li(Si)/FeS_2 and Li(Si)/CoS_2 cells, respectively, for unflooded anodes. For the FeS_2 cells (Figure 11), the hump in the resistance curves at ~130 s is a result of the higher resistivity of the first discharge phase, $Li_3Fe_2S_4$. The rapid rise in resistance near the end of the discharge is most likely related to concentration polarization. The all-Li cell showed the best results.

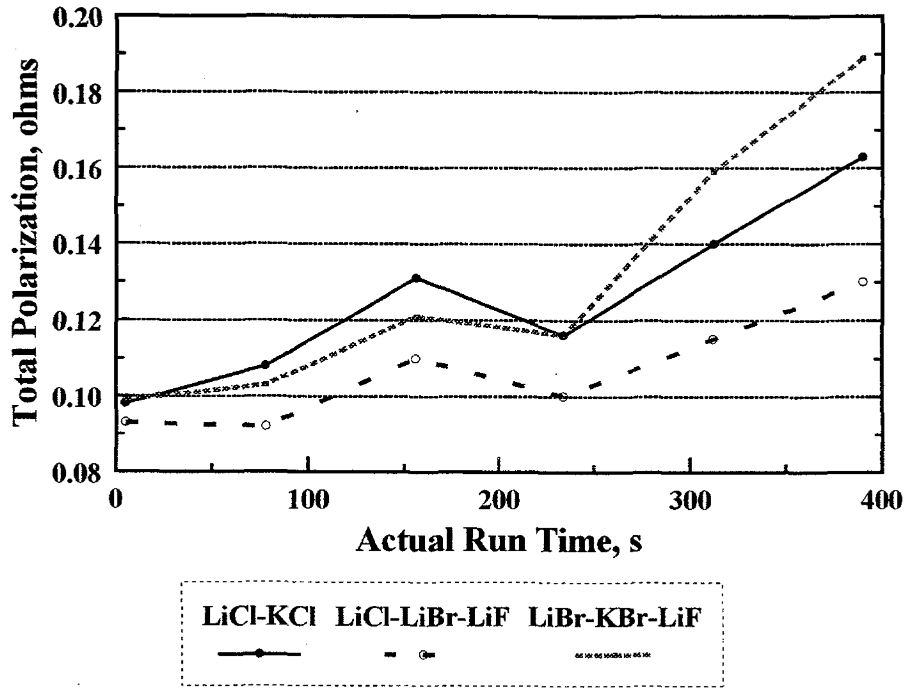

Figure 10. Total Polarization during Pulse for Single Cells Tested at 450°C for Various Electrolytes for FeS_2-Based Catholyte.

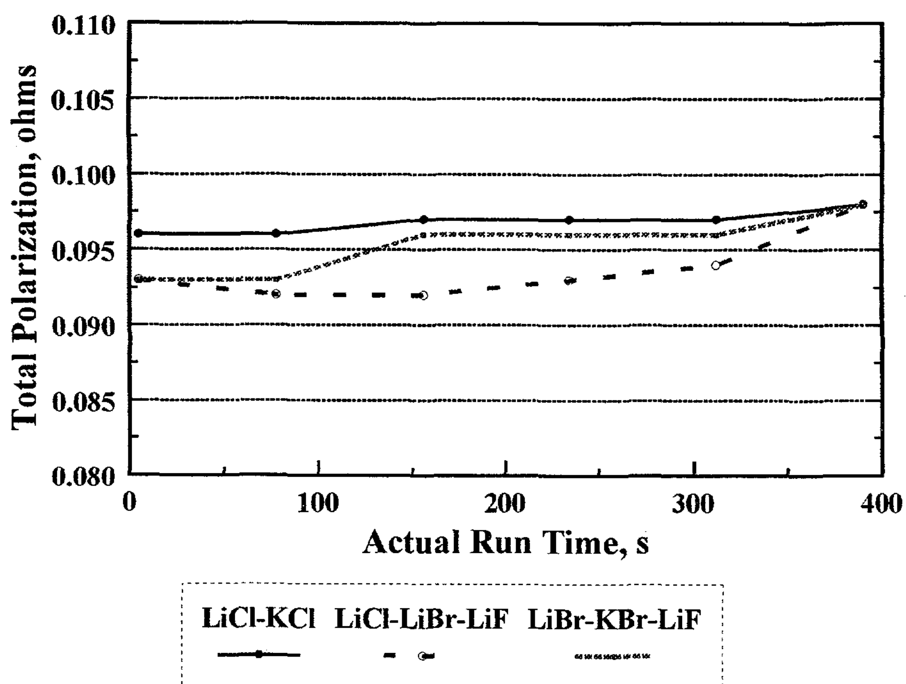

Figure 11. Total Polarization during Pulse for Single Cells Tested at 450°C for Various Electrolytes for CoS_2-Based Catholyte.

The results for CoS_2 cells (Figure 12) are in marked contrast with those of the FeS_2 cells (Figure 10). The polarization-time profiles were flat for all the electrolytes, with the lowest values shown by the all-Li cell.

Based on the data generated for the various electrolytes, the first choice for the design application is the *<u>all-Li electrolyte</u>.*

Cathode Effects – The performance of FeS_2 cathode was impacted by the electrolyte used, while that of the CoS_2 cathode was not affected nearly as much. The relative differences in the maximum pulse currents for FeS_2 and CoS_2 at 450°C are shown in Figures 12, 13, and 14 for the standard LiCl-KC1, the all-Li, and the low-melting electrolytes, respectively, for standard anodes. CoS_2 greatly outperformed FeS_2 when the standard LiCl-KC1 eutectic was used (Figure 12). The CoS_2 was able to sustain the 9-A pulse current for 234 s, while the FeS_2 lasted only 78 s. The relative differences were not as great, however, when the superior all-Li electrolyte was used (Figure 13). Both cathodes were able to sustain the 9-A pulse current for 234 s, although the pulse current delivered by the CoS_2 was still higher than that for the FeS_2 for the duration or the run. The performance of the low-melting electrolyte (Figure 14) was intermediate between that of the LiCl-KC1 and all-Li electrolytes. These trends were evident at higher temperatures, as well.

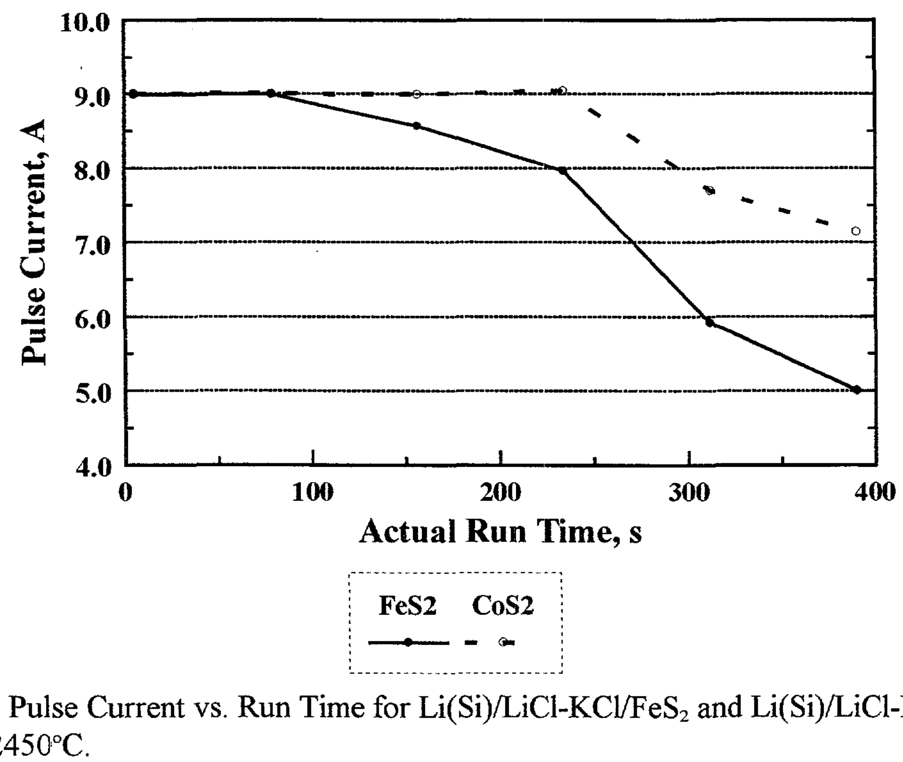

Figure 12. Pulse Current vs. Run Time for Li(Si)/LiCl-KCl/FeS_2 and Li(Si)/LiCl-KCl/CoS_2 Cells Tested at 2450°C.

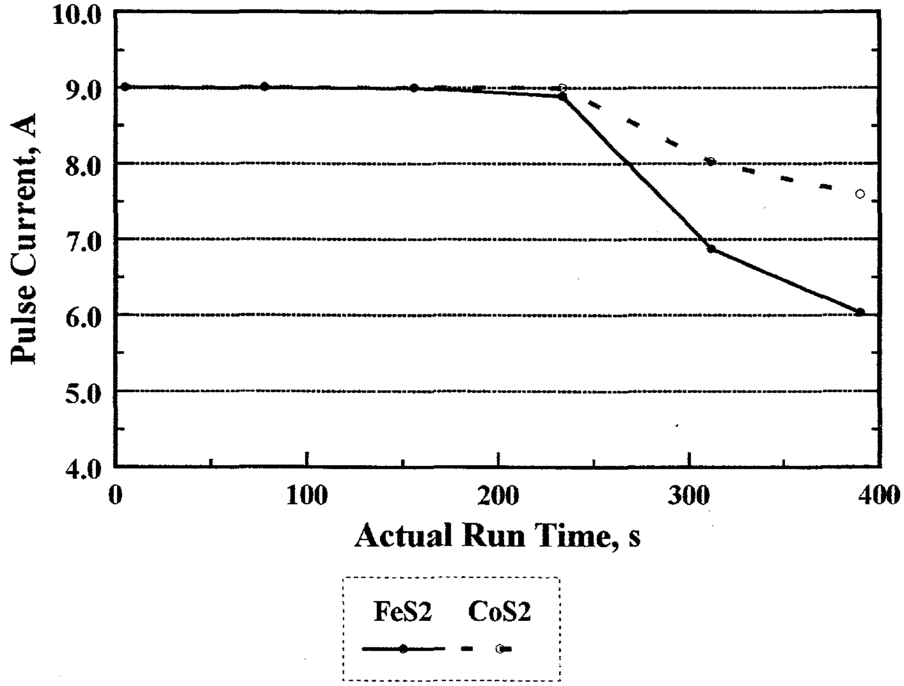

Figure 13. Pulse Current vs. Run Time for Li(Si)/LiCl-LiBr-LiF/FeS_2 and Li(Si)/LiCl-LiBr-LiF/CoS_2 Cells Tested at 450°C.

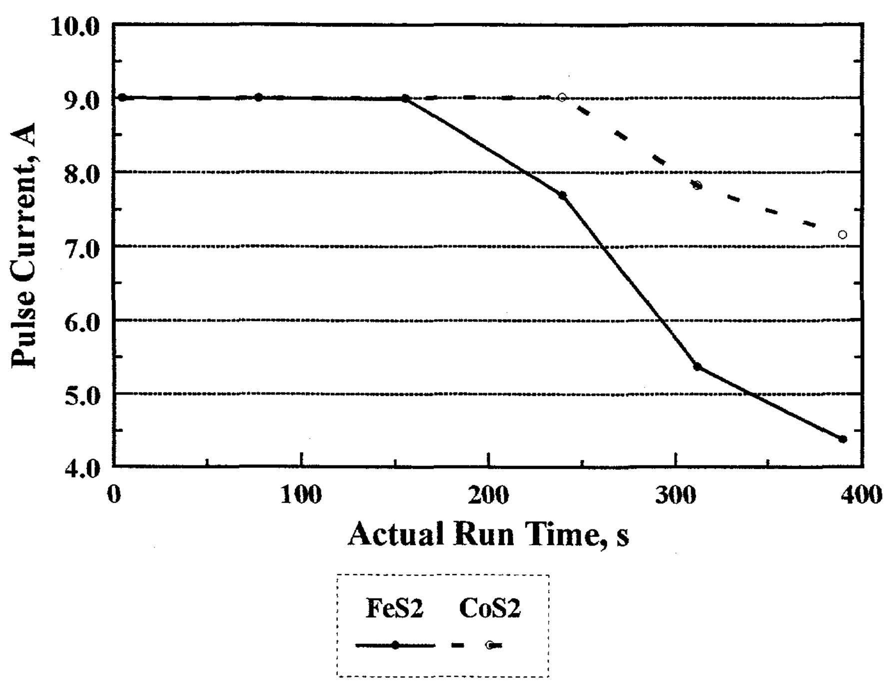

Figure 14. Pulse Current vs. Run Time for Li(Si)/LiBr-KBr-LiF/FeS_2 and Li(Si)/LiBr-KBr-LiF/CoS_2 Cells Tested at 450°C.

The relative differences in the total polarization for the Li(Si)/ FeS_2 and Li(Si)/CoS_2 cells at 450°C are shown in Figures 15, 16, and 17 for the standard LiCl-KC1, the all-Li, and low-melting electrolytes, respectively, for standard (unflooded) anodes. In all cases, the cell polarization for the CoS_2 cells was much lower than that for the FeS_2 cells. It is significant that the polarization for the CoS_2 cells did not change much as a function of depth of discharge, while that for FeS_2 cells rose dramatically under the same conditions. The magnitude of the hump in the polarization curve for the FeS_2 cells decreased with increase in temperature. The relative differences in performance were similar for all the electrolytes, except that the absolute value of the resistance for the FeS_2 cells was much lower with the all-Li electrolyte (Figure 17).

The open-circuit voltage of the Li(Si)/FeS_2 cell at 450°C is about 100 mV higher than that of the Li(Si)/CoS_2 cell. However, its lower cell resistance and greater rate capability make up for this shortly into the discharge. This is evident in Figures 18, 19, and 20 which show the minimum pulse voltage for the two cells at 450°C for the LiCl-KC1, all-Li, and low-melting electrolytes for standard anodes. The FeS_2 cell had a higher minimum pulse voltage than the CoS_2 cell at about 50 s when the LiCl-KC1 electrolyte was used (Figure 18). In the case of the all-Li electrolyte (Figure 19), the crossover point occurred near 100 s. The CoS_2 cell outperformed the FeS_2 cell for the entire run when the low melting electrolyte was used (Figure 20). Similar electrolyte effects were observed at higher temperatures.

Based on the data generated for the two cathodes, the first choice for the design application is <u>*CoS_2*</u>. This material has a thermal stability limit that is 100°C higher than that of FeS_2 and has a greater rate capability and lower internal resistance. However, since its open-circuit voltage is about 100 mV less than that for FeS_2, a tradeoff must be made if severe height constraints are imposed.

Flooded Anodes – The use of flooded anodes (with free electrolyte added) improved the performance of the Li(Si)/FeS_2 cells with the LiCl-KCl eutectic at temperatures of 450°C or greater, compared to unflooded anodes. However, the effects were minimal with the other electrolytes and with the Li(Si)/CoS_2 cells. The effect on the minimum pulse voltage is shown in Figures 21 and 22 at a temperature of 450°C for Li(Si)/FeS_2 and Li(Si)/CoS_2 cells, respectively, for the LiCl-KC1 eutectic.

Even if the effect on electrochemical performance is not substantial in all cases, the incorporation of free electrolyte reduces the pressure necessary for pelletizing, increases the pellet yields, and reduces galling of the pelletizing dies. The loss in capacity incurred by using the electrolyte additive in the anode is made up by the higher density of the anolyte. The net result is that the capacities are virtually the same for the same thickness of pellet for both anode materials. Consequently, flooded anodes should be used in the final battery design to take advantage of the enhanced mechanical properties of the pellets.

Single-Cell Recommendations – *Based on the results of the single-cell screening tests, the first choice for the design application is the* <u>*Li(Si)-LiCl-LiBr-LiF/CoS_2*</u> *system and* <u>*flooded anodes*</u>. The low-melting system is the next best choice, since it performed adequately and required less heat input than the all-Li and standard LiCl-KC1 eutectics. This would reduce the effective stack

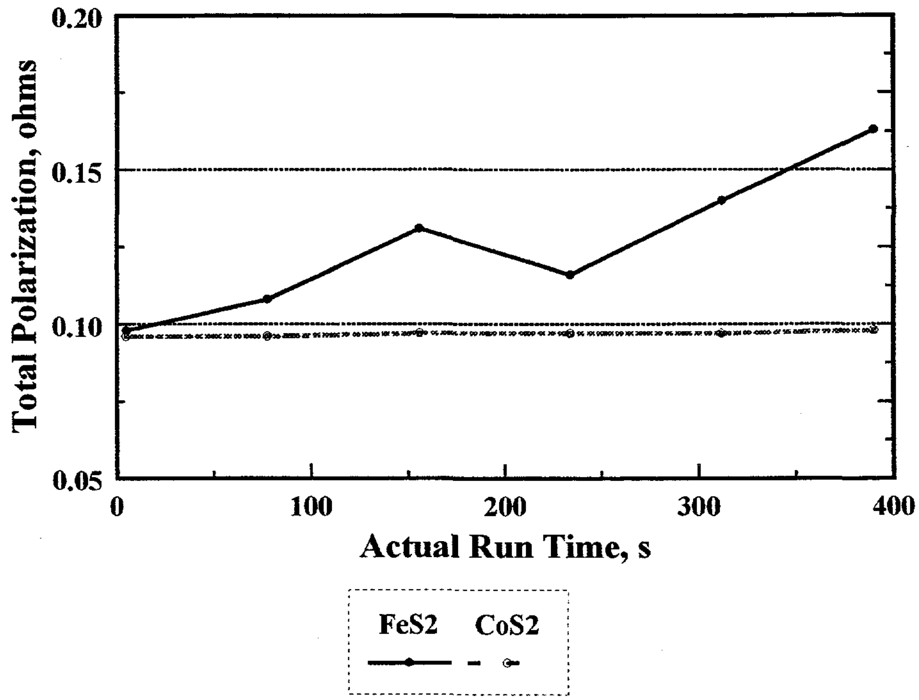

Figure 15. Total Polarization vs. Run Time for Li(Si)/LiCl-KCl/FeS_2 and Li(Si)/LiCl-KCl/CoS_2 Cells Tested at 450°C.

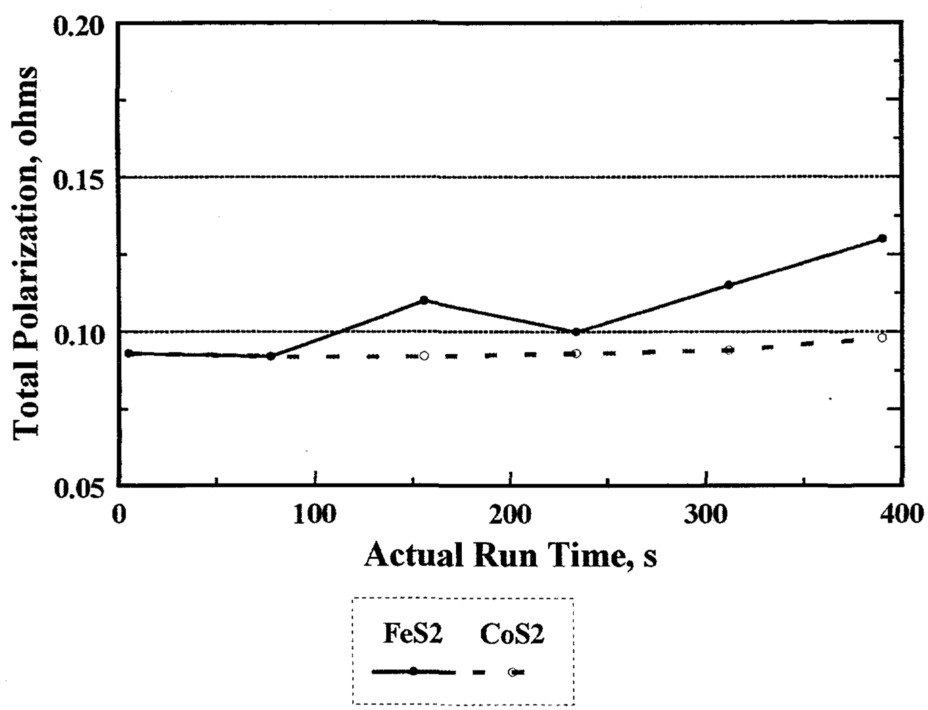

Figure 16. Total Polarization vs. Run Time for Li(Si)/LiCl-LiBr-LiF/FeS_2 and Li(Si)/LiCl-LiBr-LiF/CoS_2 Cells Tested at 450°C.

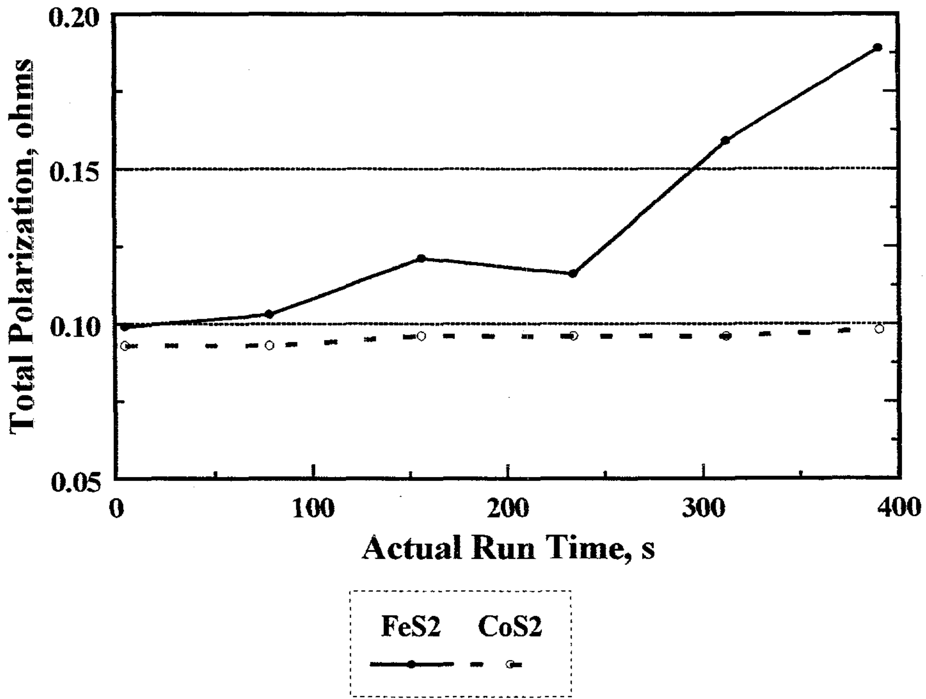

Figure 17. Total Polarization vs. Run Time for Li(Si)/LiBr-KBr-LiF/FeS_2 and Li(Si)/LiBr-KBr-LiF/CoS_2 Cells Tested at 450°C.

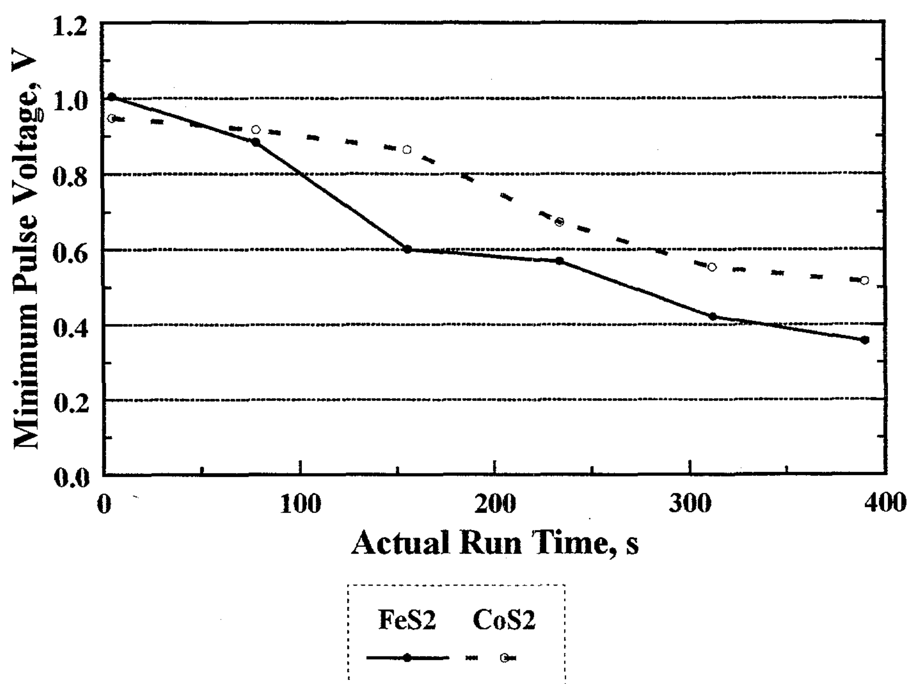

Figure 18. Minimum Pulse Voltage Run Time for Li(Si)/LiCl-KCl/FeS_2 and Li(Si)/LiCl-KCl/CoS_2 Cells Tested at 450°C.

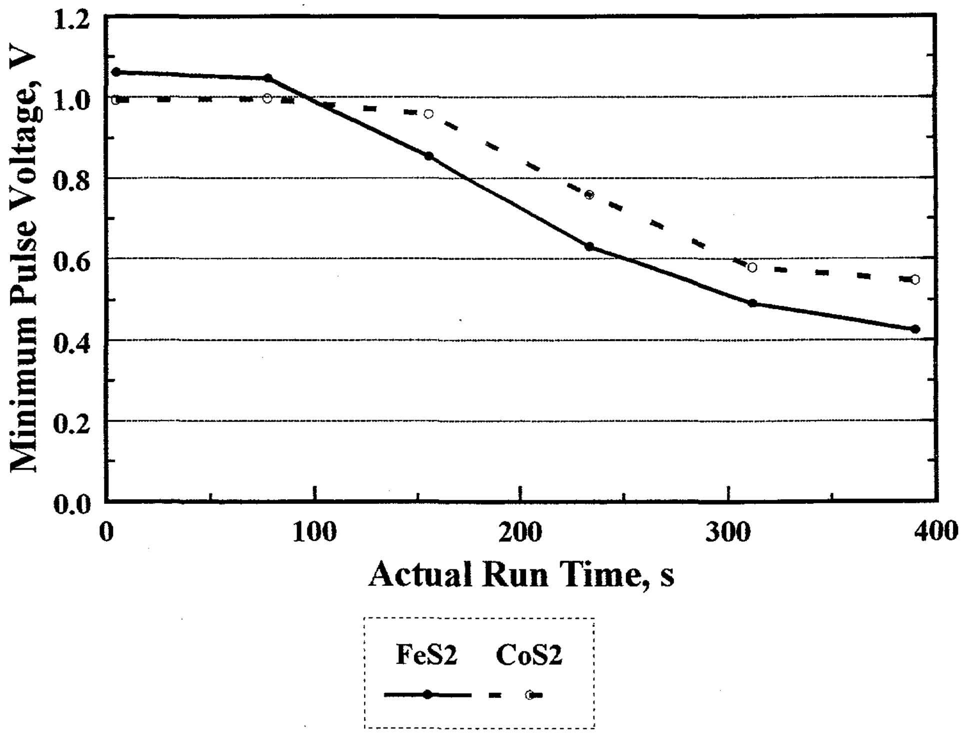

Figure 19. Minimum Pulse Voltage Run Time for Li(Si)/LiCl-LiBr-LiF/FeS_2 and Li(Si)/LiCl-LiBr-LiF/CoS_2 Cells Tested at 450°C.

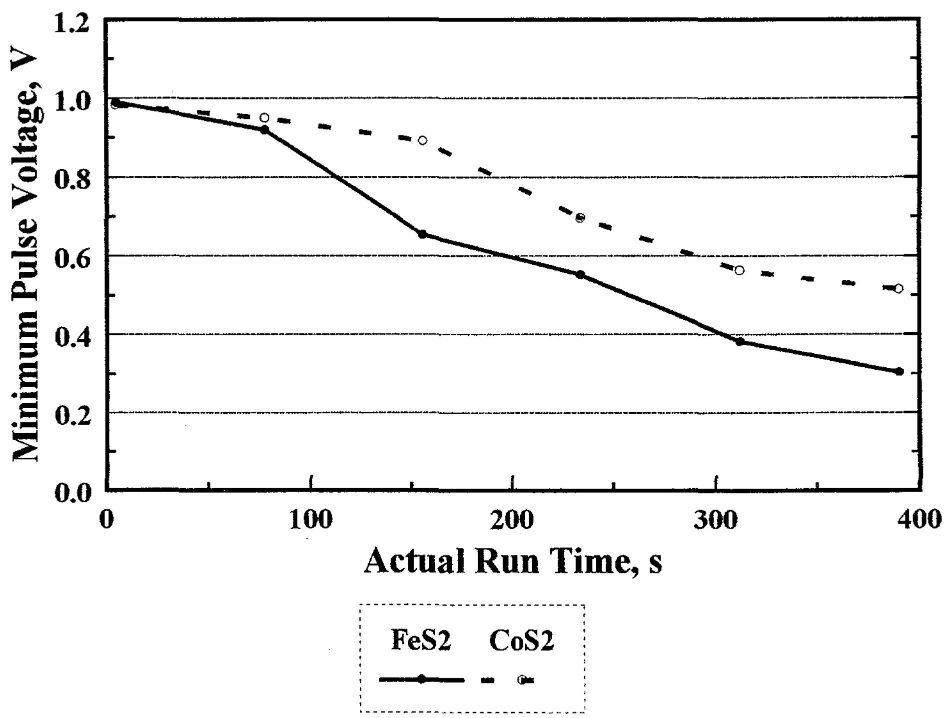

Figure 20. Minimum Pulse Voltage Run Time for Li(Si)/LiBr-KBr-LiF/FeS_2 and Li(Si)/LiBr-KBr-LiF/CoS_2 Cells Tested at 450°C.

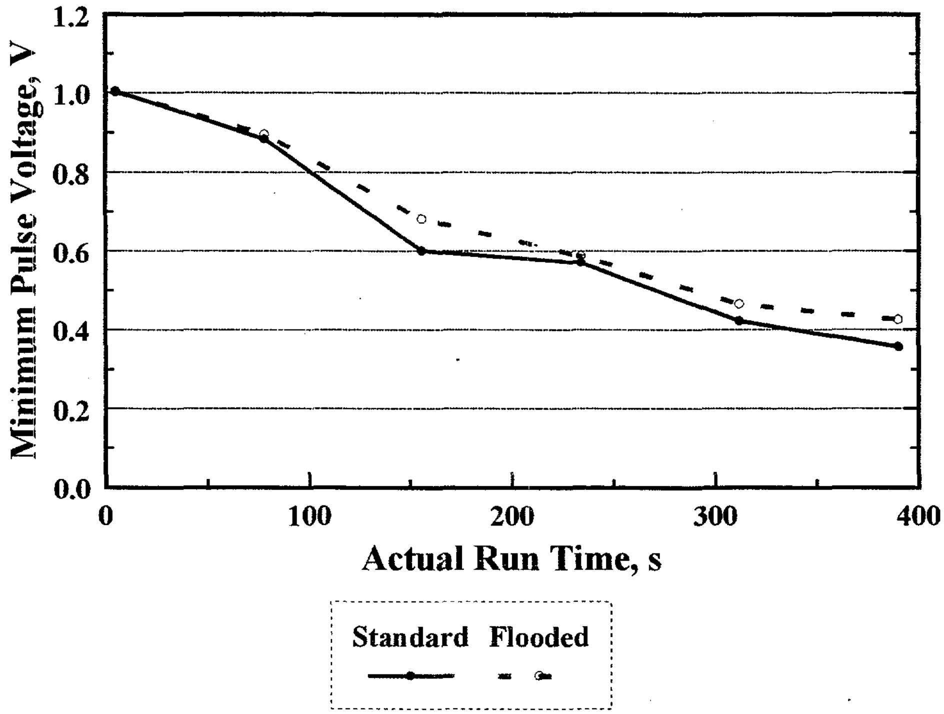

Figure 21. Effect of Flooded Anodes on the Minimum Voltage During Testing of Li(Si)/LiCl-KCl/FeS_2 Cells at 450°C.

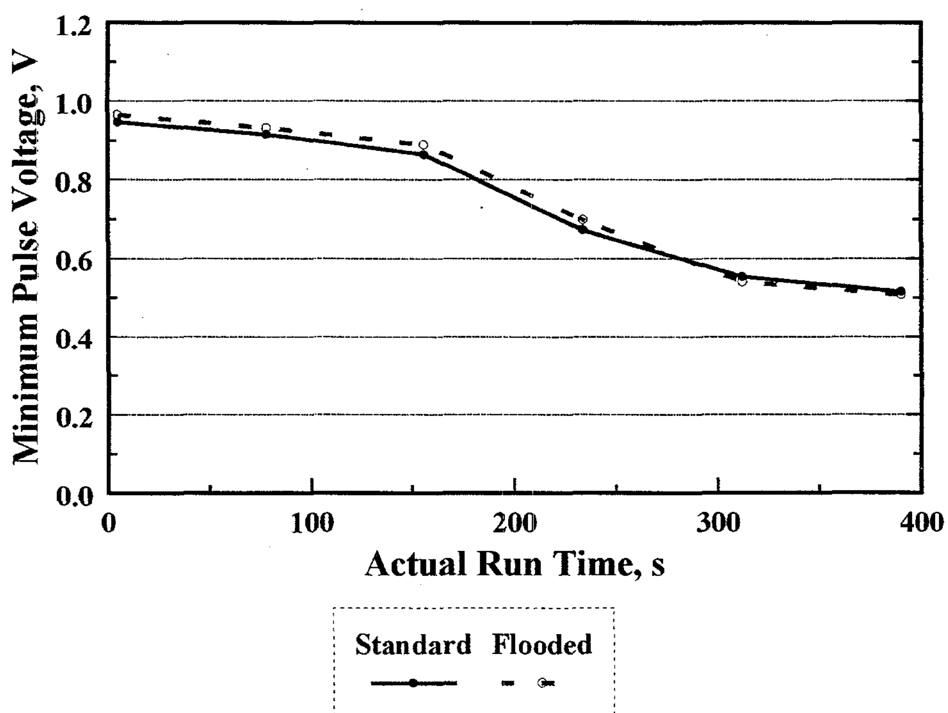

Figure 22. Effect of Flooded Anodes on the Minimum Voltage During Testing of Li(Si)/LiCl-KCl/CoS_2 Cells at 450°C.

height and would allow more cells to be used in place of the space taken by the heat pellets for the all- Li system.

Battery Tests

During the testing process, several changes were made to the way in which the batteries were tested, because of lack of adequate time to finish a full matrix of tests as was initially desired. Most of the units were tested using the R&D tester, which was the unit where most of the software changes were made. Several batteries were also tested with the tester of our sister battery group. Because of differences in the way the data are acquired for the two testers, a one-to-one comparison of data from the two testers was not always possible. However, the differences were such that meaningful comparisons were still generally possible.

Fiberfrax® Insulation – Several 10- and 25-cell batteries insulated with Fiberfrax® were tested using the all-Li electrolyte. All the batteries were instrumented with a thermocouple in the stack in the last cell from the header end. Both 1.25"-dia. and 2.25"-dia. batteries were tested. The heat balance ranged from 98-109 cal/g for these tests. The data from these tests are summarized in Table 3.

For the CoS_2 batteries, peak stack temperatures of 435° to 486°C were observed for the cold (-54°C) batteries for heat balances of 98 to 109 cal/g. Peak stack temperatures of 530° to 560°C were observed for the corresponding hot (74°C) batteries. These data indicate that the highest heat balance of 109 cal/g is low. (Normal peak stack temperatures of 520° to 540°C are typical for a properly balanced battery activated cold and 550°- to 580°C for one activated hot.) The nominal peak voltage for a 100-cell Li(Si)/CoS_2 battery would be between 181 and 183 V for a heat balance of 109 cal/g. (Note that the emf of the Li(Si)/CoS_2 system is not very sensitive to temperature because of the small entropy for the discharge reaction.) The minimum voltage that the 100-cell battery would experience under these conditions is estimated to be 125-135 V.

Problems were encountered in testing of the batteries with FeS_2 cathodes. The first difficulties were observed at a heat balance of 104 cal/g for a 10-cell, 2.25" dia. battery activated under hot conditions. The battery performance appeared fine initially and the peak temperature was normal (540°C). However, after 85 s, the battery went into thermal runaway. A later test with 10-cell, 1.25"-dia. battery also ended with thermal runaway.

Several issues were considered to try to understand the causes of the thermal runaway behavior of the Li(Si)/FeS_2 batteries. Potential causes of the thermal runaway are:

- Anode ignition caused by thin cells
- Shorting of cells by thermocouple
- Shorting of cells by chips from anode or cathode
- High rate of heat input to cathode interface

The first three scenarios would not be unique to the FeS_2 batteries; such factors would be equally present for the CoS_2 batteries. The last factor appears the most logical causative effect for thermal runaway and relates to the relative thermal stability of the FeS_2 and CoS_2. The fourth factor dealing with rate of heat input is also coupled with the thickness of the cells and

Table 3. Summary of Results of Tests of 10- and 25-Cell Li(Si)/LiCl-LiBr-LiF/CoS_2 Batteries Built with Fiberfrax® Insulation.#

Cathode	Activ. Temp., °C	Heat Bal., cal/g	No. Cells	Dia., in	Temperature Range, °C	Res. @ 300 s, ohms
CoS_2	-54	98	10	1.25	435-->420	1.888
CoS_2	74	98	10	1.25	530-->490	0.201
CoS_2	-54	98	10	2.25	443-->434	0.373
CoS_2	74	98	10	2.25	536-->503	0.100
CoS_2	26	102	10	1.25	544-->472	0.172
CoS_2	74	109	10	2.25	560-->550	0.104
CoS_2	-54	109	10	2.25	485-->455	0.080
FeS_2	74	98	10	2.25	530-->483	0.128
FeS_2	74	104	10	1.25	Battery burned up	
FeS_2	74	109	10	2.25	Battery burned up	
FeS_2	74	106	10	2.25	550-->510	0.123
CoS_2	74	106	25	2.25	568-->543	0.258
CoS_2	-54	106	25	2.25	475-->460	0.252
FeS_2	74	104	25	2.25	540-->1080	Battery burned up
FeS_2	-54	104	25	2.25	470-->431	1.703

84/16 heat powder.

the width of the heat-paper strip used to ignite the individual heat pellets in the stack. Thicker cathode cells have more mass that can dissipate the heat generated by the burning heat-paper strip. Battery burn-up is not as likely with CoS_2 as with FeS_2 since CoS_2 can be heated to a much higher temperature—about 650°C vs. 550°C for FeS_2.

The width of the heat-paper strip was suspected to be the primary factor for our thermal-runaway problem. That is schematically illustrated in Figure 23. Localized overheating is suspected to be the culprit. Batteries with FeS_2 cannot sustain localized overheating as well as CoS_2 because of the lower thermal stability of FeS_2. This premise was tested in 10-cell batteries where a 1/8"-wide heat-paper strip was used in place of the normal ¼"-wide strip. No ignition occurred at heat balances of 104 cal/g (as was observed previously), 106 cal/g, and 109 cal/g. All future battery tests employed the thinner heat-paper ignition strips and further thermal-runaway problems were not encountered.

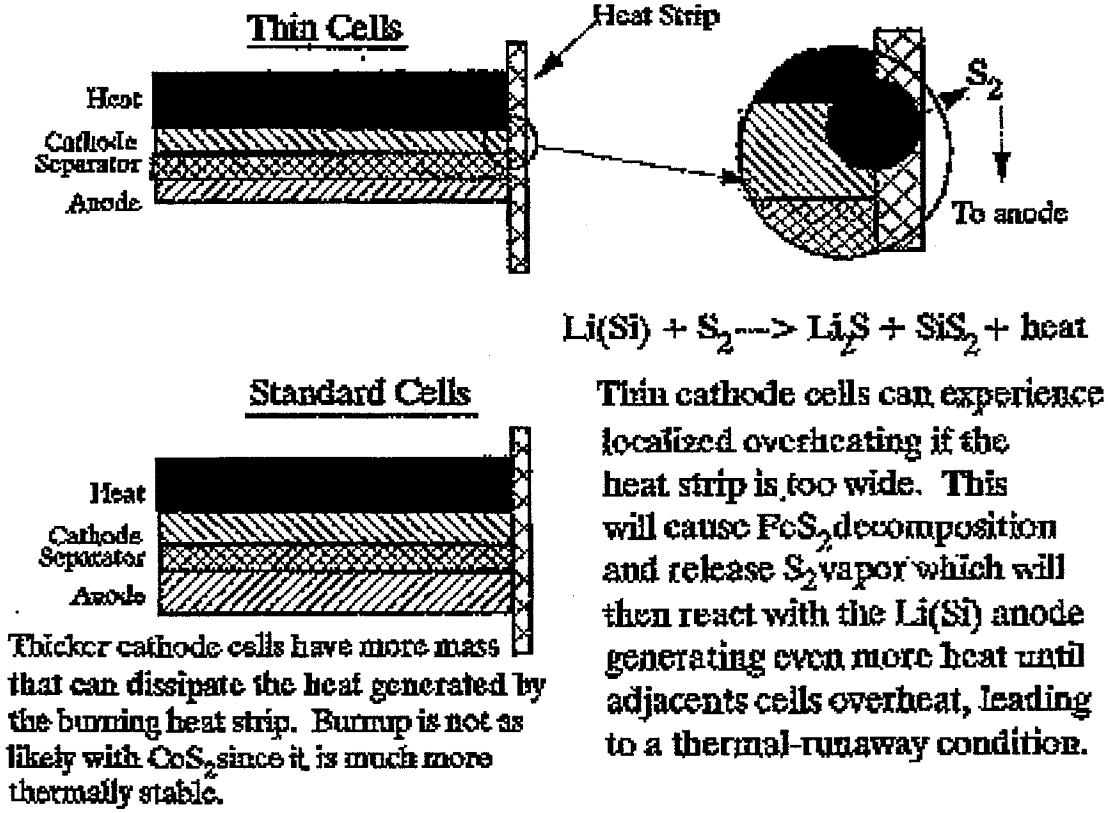

Figure 23. Schematic Representation of Possible Mechanism that Could Result in Thermal-Runaway Condition in Li(Si)/FeS_2 Battery.

Based on the initial data for the 2.25"-dia. FeS_2 batteries, a heat balance of more than 109 cal/g is indicated for optimum performance for batteries insulated with Fiberfrax®. The heat balance for Li(Si)/FeS_2 batteries are generally higher than the corresponding Li(Si)/CoS_2 design. The initial peak voltages for the FeS_2 batteries would be higher than those for the CoS_2 batteries. At the minimum pulse voltage at 300 s, however, they would be lower because of the higher internal cell resistance of the FeS_2 batteries.

Min-K® Insulation – Parallel tests with 2.25"-dia., 25-cell batteries with the all-Li electrolyte were also conducted using Min-K® insulation in place of the Fiberfrax® wrap. For comparison purposes, tests with the low-melting (LiBr-KBr-LiF) electrolyte were also included. (The heat balance will be somewhat lower using Min-K® because of its superior insulating properties.) The results of the tests are summarized in Table 4; the battery stack was not thermocoupled for these tests.

The best results to date with FeS_2 and the all-Li electrolyte were obtained at a heat balance of 105 cal/g (25-cell batteries). The data suggest that an even higher heat balance would be necessary for this combination--closer to 108 cal/g. The battery resistance for the hot battery was 0.203 ohms and the minimum voltage for a 100-cell battery is projected to be 107.4 V.

Table 4. Summary of Results of 10- and 25-Cell Tests with Min-K® Insulation.*

Cathode	Temp., °C	Heat Bal., cal/g	No. Cells	Tester	Res. @ 300s, ohms	V_{min} @ 300s for 100 Cells, V
			All-Li Electrolyte			
CoS_2	74	85	10	BTG@	N.A.#	157.5
CoS_2	-54	85	10	BTG	N.A.	N.A.
CoS_2	74	90	10	BTG	N.A.	155.3
CoS_2	-54	90	10	BTG	N.A.	144.4
CoS_2	74	101	25	R&D	0.171	134.7
CoS_2	-54	101	25	R&D	0.666	69.18
FeS_2	74	92.3	10	BTG	N.A.	157.4
FeS_2	-54	92.3	10	BTG	N.A.	125.6
FeS_2	74	95	10	BTG	N.A.	169.3
FeS_2	-54	95	10	BTG	N.A.	128.3
FeS_2	74	101	25	R&D	0.155	51.18
FeS_2	-54	101	25	R&D	0:564	6.85
FeS_2	74	105	25	R&D	0.203	107.4
			Low-Melting Electrolyte			
CoS_2	74	50	10	BTG	N.A.	157.4
CoS_2	-54	80	10	BTG	N.A.	148.2
CoS_2	74	85	10	BTG	N.A.	157.1
CoS_2	-54	85	10	BTG	N.A.	152.9
CoS_2	74	88	25	R&D	0.215	126.2
CoS_2	-54	88	10	R&D	0.146	106.6
FeS_2	74	90	10	BTG	N.A.	137.2
FeS_2	-54	90	10	BTG	N.A.	148.4
FeS_2	74	95	10	BTG	N.A.	129.0
FeS_2	-54	95	10	BTG	N.A.	151.1

* 84/16 heat; 2.25"-dia. stack.

N.A. = Not available.

@ BTG = Battery Test Group.

In contrast, the battery resistance for the CoS_2 batteries with the all-Li electrolyte at a heat balance of 101 cal/g—the highest heat balance studied with Min-K® insulation—was 0.171 ohms under the same discharge conditions, with the minimum pulse voltage for 100 cells projected to be 134.7 V. The high resistance of 0.666 ohms for the cold battery indicates that the optimum heat balance for the CoS_2 battery using the all-Li electrolyte would be greater than 101 cal/g—probably closer to 105 cal/g.

When the low-melting electrolyte was substituted for the all-Li electrolyte, the required heat balance was greatly reduced--only 88 cal/g for the CoS_2 system and 90-95 cal/g for the FeS_2 system. For FeS_2, the peak voltage of 100-cell batteries would be greater than' for the CoS_2 counterparts. However, the minimum pulse voltage would be much less because of the larger resistance of the FeS_2 cells. This trend was also noted for the all-Li system.

Several transitions were observed in the cell voltage during discharge. The initial one was related to the anode and the second one was related to the cathode. To minimize these transitions, the capacities of the anode and cathode were increased by increasing the pellet weights. The flooded-anode weight was increased from 1.45 g to 1.89 g for the 2.25"-dia. pellets. As shown in Figure 24 for FeS_2 batteries built with the all-Li electrolyte, the heavier anode removed the first transition.

The cathode weight was next increased from 2.48 g to 3.13 g. The effect of cathode weight is shown in Figure 25 for Li(Si)/CoS_2 batteries based in the low-melting electrolyte with the flooded, heavier (1.89 g) anodes. The steady-state voltage was raised considerably between 300 and 450 s. However, since this is outside of the lifetime requirements for the battery, the use of the heavier cathode for the HVHP application would not appear necessary. The heavier anode, however, did improve the performance during this same period.

95-Cell Test – Enough material and time remained in the study to build and test a 95-cell Li(Si)/CoS_2 battery based on the low-melting LiBr-KBr-LiF eutectic using the heavier anodes and cathodes (1.89 g and 3.13 g, respectively). The stack diameter was 2.25-in. and the heat balance was 88 cal/g. The battery was tested under hot conditions (74°C) using the 4-kW electronic load modules.

The steady-state battery voltage is shown as a function of time in Figure 26. The battery was pulsed from a steady-state current of 6 A to 36 A every 2 s; using a pulse width of 43 ms. The performance was quite good, considering that the load used for this test was really designed to be used with a 2.5"-dia. stack.

The minimum pulse voltage for the tests is shown in Figure 27. At the design life of the battery of 300 s, the minimum battery voltage was 139.5 V while under the 36-A pulse load.

The total polarization versus time is plotted in Figure 28. It remained fairly constant, except for the small hump near 400 s because of the increase in the resistance of the first discharge phase.

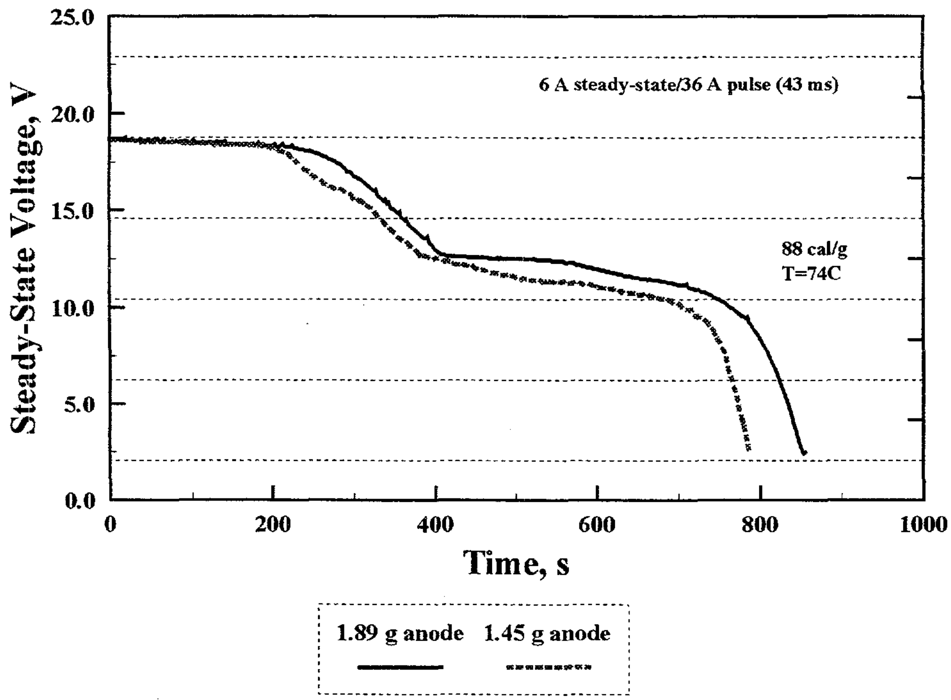

Figure 24. Effect of Anode Weight on the Discharge of 25-Cell Li(Si)/LiCl-LiBr-LiF/FeS_2 Thermal Batteries.

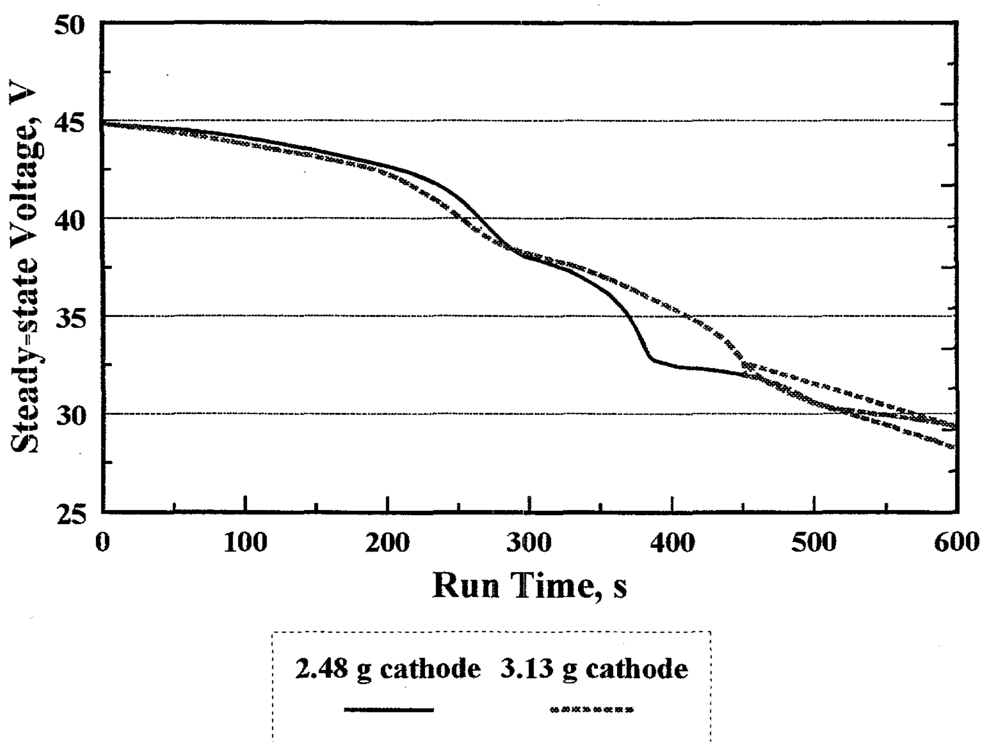

Figure 25. Steady-State Voltage of 25-Cell Li(Si)/LiBr-KBr-LiF/CoS_2 Thermal Battery Built with Flooded Anodes.

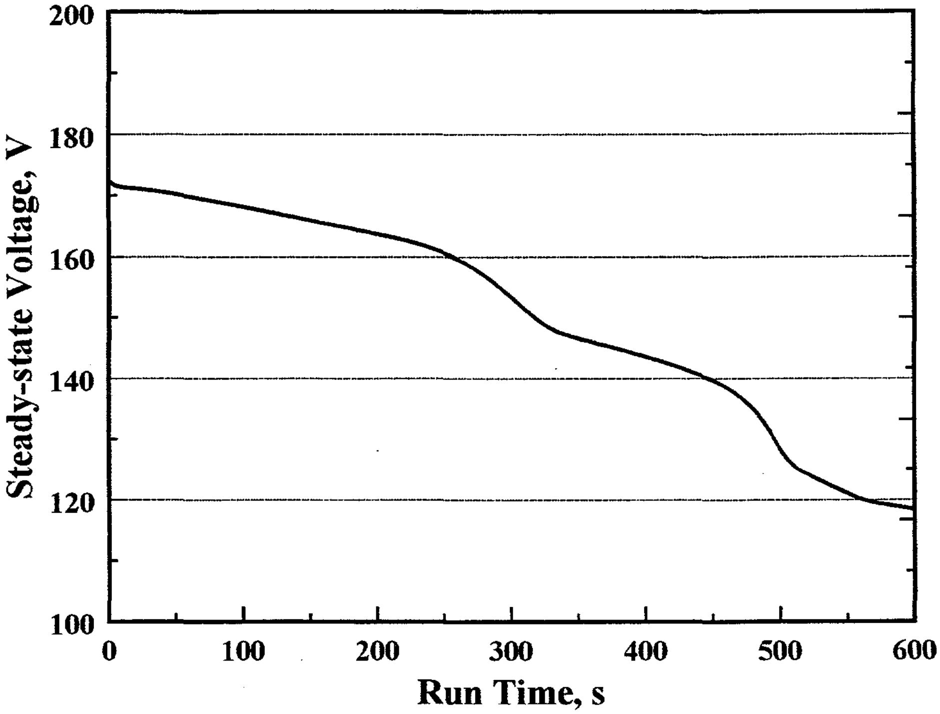

Figure 26. Steady-State Voltage of 95-Cell Li(Si)/LiBr-KBr-LiF/CoS_2 Thermal Battery Built with Flooded Anodes.

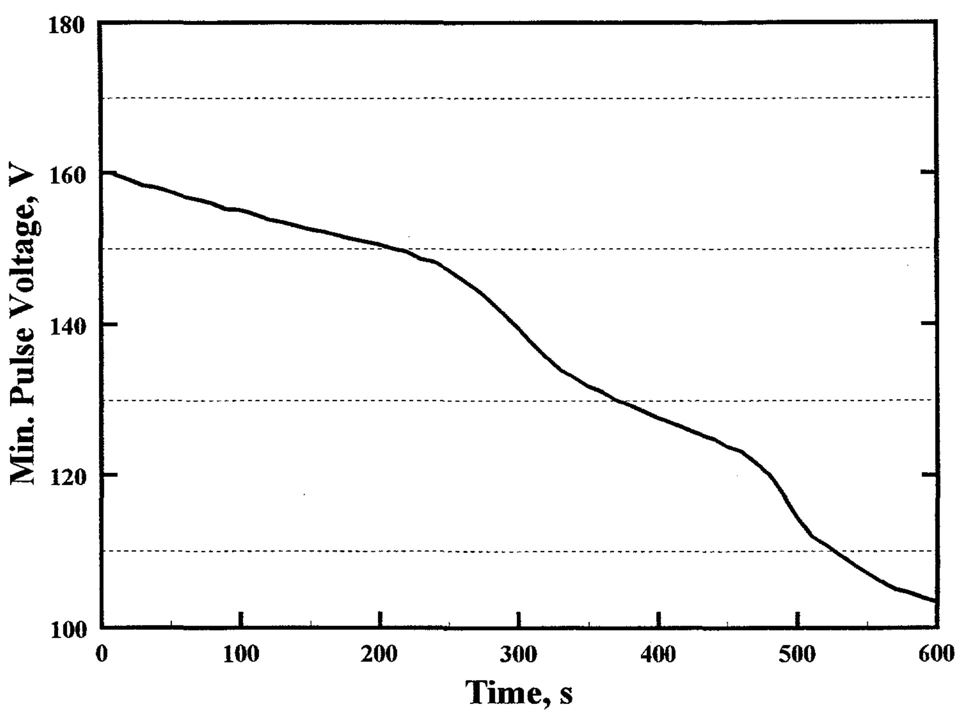

Figure 27. Minimum Pulse Voltage of 95-Cell Li(Si)/LiBr-KBr-LiF/CoS_2 Thermal Battery Built with Flooded Anodes.

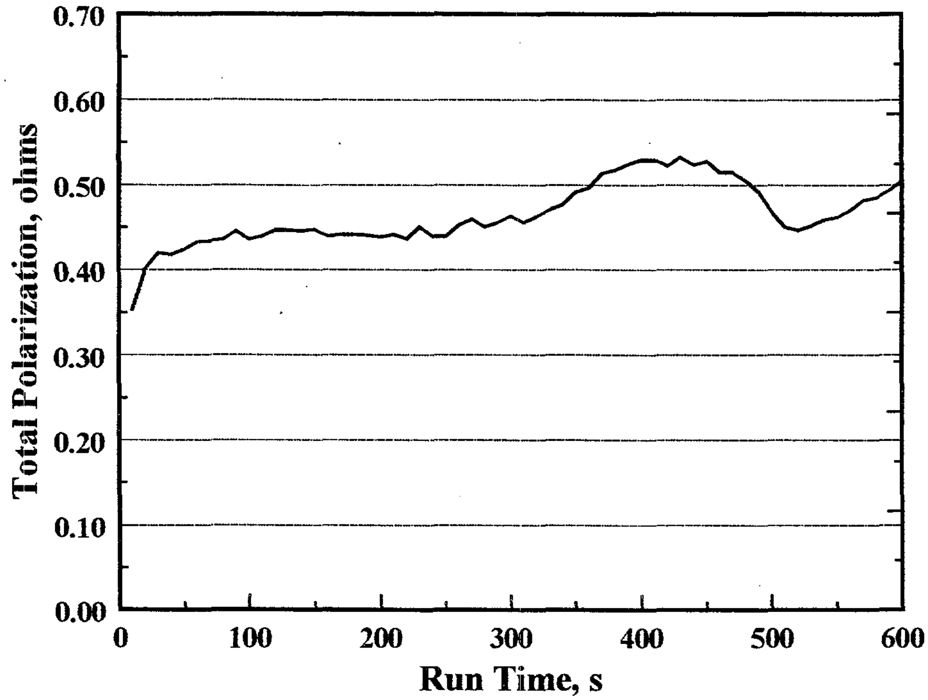

Figure 28. Total Polarization of 95-Cell Li(Si)/LiBr-KBr-LiF/CoS_2 Thermal Battery Built with Flooded Anodes.

The relative performance of the 25-cell and 95-cell batteries can be more readily compared when the parameters are normalized to the cell level. The steady-state voltages on a per-cell level are plotted in Figure 29. The results for the 95-cell battery were better than predicted based on the data for the 25-cell battery. This type of improvement upon scaleup of battery size is typical.

The minimum pulse voltage on a per-cell basis is shown in Figure 30. The same trend observed for the steady-state voltage was exhibited by the minimum pulse voltage: the larger battery performed better. The reason for the improved performance of the larger battery is the lower resistance. This is shown in Figure 31 where the average resistance per cell is compared for the two batteries. The per-cell resistance for the larger battery was more consistent and lower throughout the discharge.

The relative temperature profiles of the external skin temperatures are plotted in Figure 32. The thermocouple was located midway between the top and bottom of the battery. The skin temperature was lower for the larger battery for the design lifetime of 300 s.

FeS_2 Comparison – A test was conducted with an off-the-shelf Li(Si)/FeS_2 thermal battery that had the same stack diameter as the 25- and 95-cell batteries (2.25-in.) but used the LiCl-KCI eutectic electrolyte. The battery had 15 cells, used Fiberfrax® wrap, and was balanced at 100 cal/g. The projected performance data for a 100-cell battery is summarized in Table 5, along with the corresponding data for a 100-cell CoS_2 battery based on KBr-LiBr-LiF eutectic.

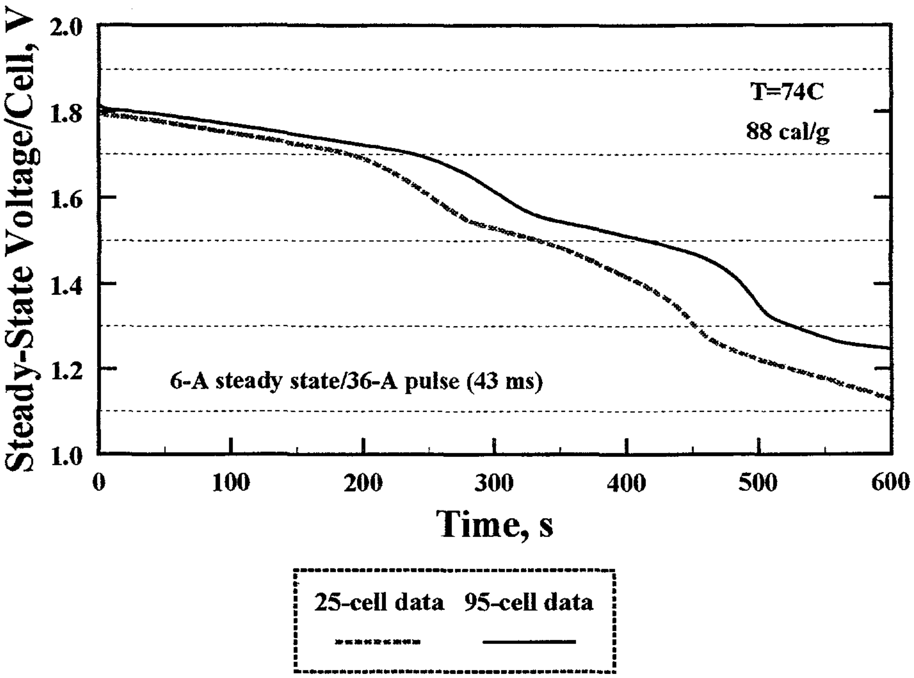

Figure 29. Comparison of Steady-State Voltage on a Per-Cell Basis for Li(Si)/LiBr-KBr-LiF/CoS_2 Thermal Batteries.

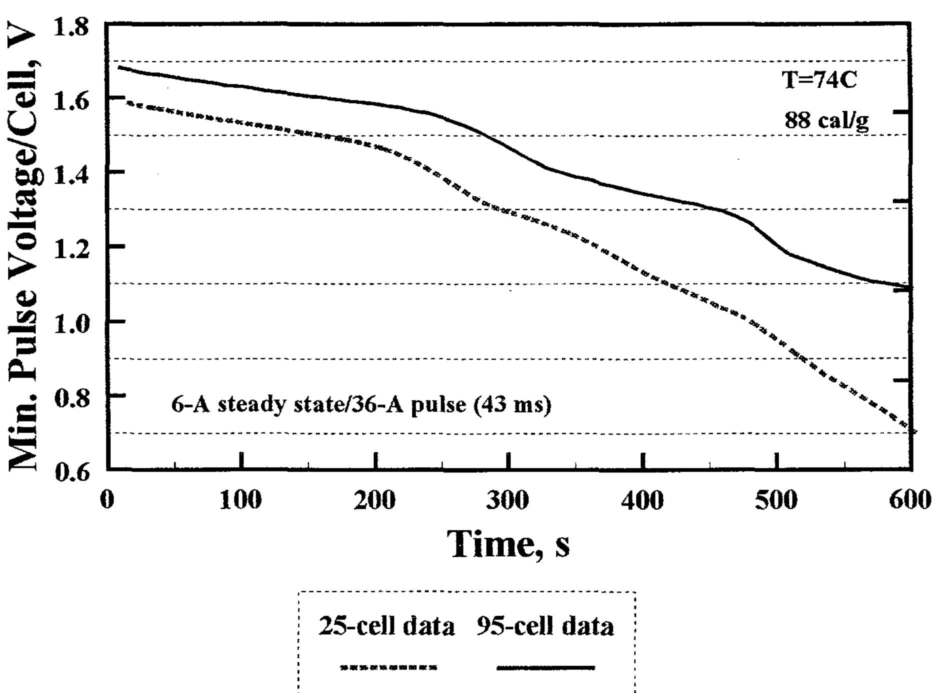

Figure 30. Comparison of Minimum-Pulse Voltage on a Per-Cell Basis for Li(Si)/LiBr-KBr-LiF/CoS_2 Thermal Batteries.

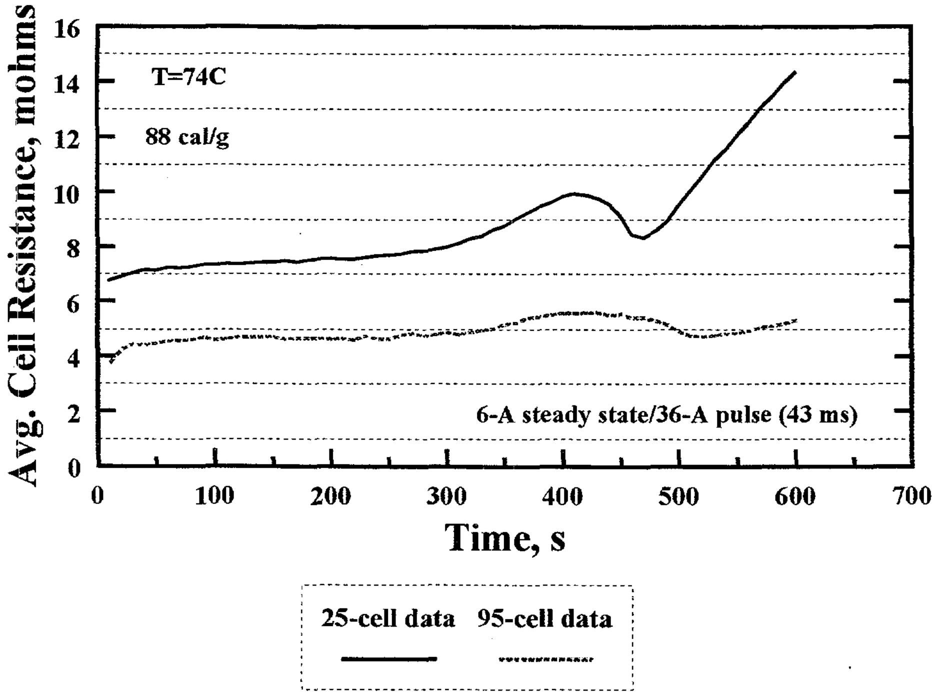

Figure 31. Comparison of Total Polarization on a Per-Cell Basis for Li(Si)/LiBr-KBr-LiF/CoS_2 Thermal Batteries.

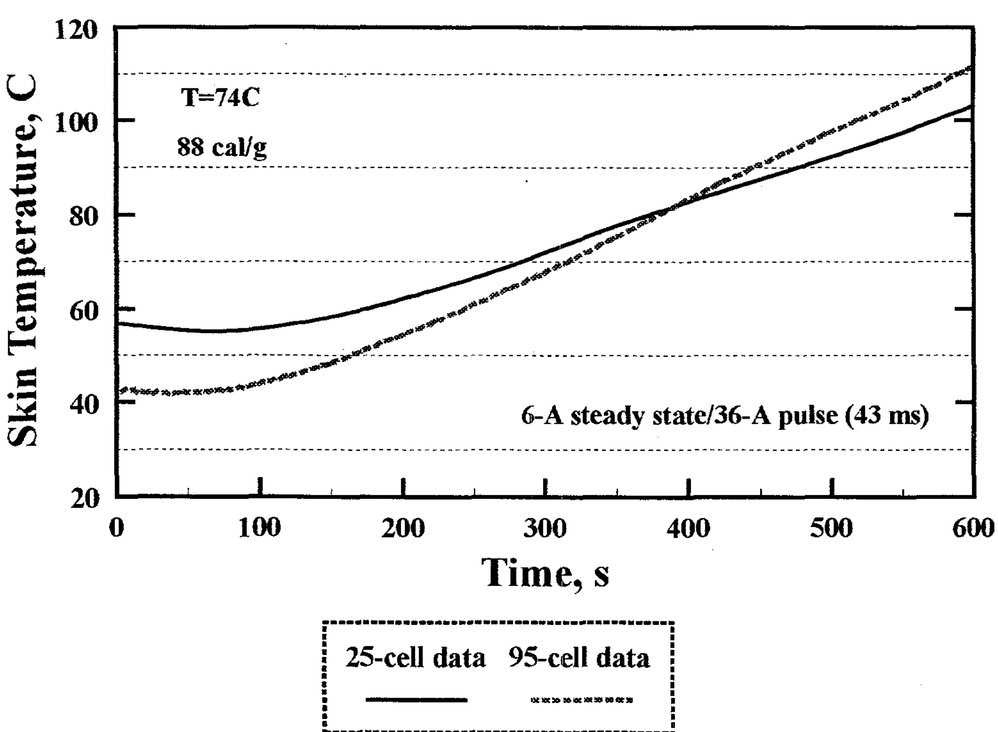

Figure 32. Comparison of Skin Temperature for Li(Si)/LiBr-KBr-LiF/CoS_2 Thermal Batteries.

Table 5. Projected Performance of 100-Cell Batteries Based on Li(Si)/LiCl-KCl/FeS_2 and Li(Si)/KBr-LiBr-LiF/CoS2 Systems.#

System	Min. Pulse Voltage at 300 s, V	Avg. Peak Battery Voltage @ 5 s, V	Resistance @ 300 s, ohms
Li(Si)/LiCl-KC1/FeS_2	146.3	196.9	1.12
Li(Si)/LiBr-KBr-LiF/CoS_2	146.9	180.6	0.490

Tested to the HVHP load profile.

The FeS_2 battery would have a much higher peak voltage, as expected because of the higher open-circuit voltage. However, the minimum pulse voltage at 300 s would be the same for the FeS_2/LiCl-KC1 and the CoS_2/low-melting system. The higher electrical conductivity of the low-melting electrolyte and CoS_2 combine to make up for the initial lower open-circuit voltage. These data corroborate the earlier single-cell screening tests with the various electrolytes comparing FeS_2 and CoS_2.

Battery-Test Recommendations – Based on the results of the 10-cell and 25-cell battery tests, the optimum heat-balance conditions are listed in Table 6.

Table 6. Optimum Heat-Balance Conditions for Li(Si)/FeS_2 and Li(Si)/CoS_2 Batteries

Insulation	Cathode	Electrolyte	Optimum Heat Balance, cal/g
Fiberfrax®	FeS_2	All-Li	109
Fiberfrax®	CoS_2	All-Li	106
Min-K®	FeS_2	Low-melting	90-95
Min-K®	CoS_2	Low-melting	88

The final design choice will be affected by volume (height) constraints faced by the engineer. The all-Li system will provide higher power than the low-melting system but will require a higher heat input. Batteries with CoS_2 have lower resistances than ones with FeS_2 but this is offset by the loss of 100 mV per cell with the former cathode. This voltage loss is mitigated later in discharge by the lower cathode resistance of CoS_2 so that the load voltage becomes higher than that for FeS_2.

CONCLUSIONS

Based on single-cell, 10-cell, and 25-cell battery tests, the Li(Si)/CoS_2 system outperforms the Li(Si)/FeS_2 system overall under the test load profile, because of the higher minimum voltage that can be delivered during pulsing after about one minute into discharge. Before this time, the FeS_2 system has a somewhat higher minimum pulse voltage. Even though the Li(Si)/CoS_2 couple has an open-circuit voltage of about 100 mV lower than that for Li(Si)/FeS_2 couple, its lower total polarization (cell resistance) more than makes up for this shortly into the discharge. This, coupled with an upper temperature window that is about 100°C higher than that for FeS_2, makes the system much safer and less likely to exhibit a thermal runaway.

Control of the thickness of the ignition strip used to fire the heat pellets is critical when FeS_2 cathodes are to be used. If the strip is more than 1/8" wide, there is an increasing tendency for localized overheating of the cathode that can initiate a thermal runaway. This was observed for certain FeS_2 batteries activated hot (74°C) using ¼"-wide heat strips. An alternative is to use a center-hole-fired design to avoid these complications.

The all-Li LiCl-LiBr-LiF eutectic electrolyte is the first choice for the intended battery application because of its superior current- and power-delivering capabilities. The low-melting LiBr-KBr-LiF eutectic is the second choice if volume (height) constraints become critical, since the heat requirements for this electrolyte are less than for the all-Li system.

The use of flooded anodes is highly recommended to facilitate the pelletization process. The use of free electrolyte reduces the forming pressure, increases pellet yields, and increases the lifetime of the dies. In some cases, flooded anodes outperform the unflooded counterparts. The presence of electrolyte also mediates the thermal shock to the cell because of the melting of electrolyte during activation. By pressing to a higher density, there is no loss in capacity with 25% free electrolyte; the same volumetric capacity can be obtained as for an unflooded anode.
The suggested heat balances for the various combinations are summarized in Table 6. It will be up to the design engineer to select the final combination after consideration of the various constraints imposed on him by the design requirements; some performance tradeoffs will be necessary.

REFERENCES

1. R. A. Guidotti and F. W. Reinhardt, "Evaluation of Alternate Electrolytes for Use in Li(Si)/FeS_2 Thermal Batteries," *Proc. 33rd Intern. Power Sources Symp.*, 369 (1988).

UNLIMITED DISTRIBUTION

2 Wright Laboratory
Aero Propulsion and Power
Directorate
Att: R. A. Marsh
D. M. Ryan
WL/POOS-2
1950 Fifth St.
Wright-Paterson AFB, OH
45433-7251

1 Argonne National Laboratory
Chemical Technology Div.
Attn: T. Kaun
9700 South Cass Ave.
Argonne, IL 604339

2 Army Research Lab
Attn: F. Krieger
A. Goldberg
2800 Powder Mill Road
Adelphi, MD. 20783

1 A. A. Benderly, Consultant
9915 Logan Dr.
Potomac, Maryland 20854

1 Boeing Aerospace
Attn: Chris Johnson
P. O. Box 3999, M/S 82-32
Seattle, WA 98199

4 Eagle-Picher Technologies, Inc.
Attn: R. Spencer
J. DeGruson
R. Hudson
C. Lamb
P.O. Box 47
Joplin, MO 64802

4 Enser Corp.
Attn: J. Ronacher
N. Shuster
N. Miller
J. Cubero
P.O. Box Drawer 48548
St. Petersburg, FL 33743-8548

1 Naval Ordnance Station
Attn: K. Englander
Code 5123C
Indian Head, MD 20640

3 Naval Surface Warfare Center
Attn: C. Winchester
P. Keller
Dr. Patricia Smith
Code 683, Electrochemistry
Branch
9500 McArthur Blvd.
W. Bethesda, MD 20817-5700

4 Naval Weapons Center
Attn: M. H. Miles
R. Nolan (Code 3626)
D. Rosenlof (Code 3626)
Carl Heiners (Code 477400D)
China Lake, Ca 93555

1 Parker Hannifin
Attn: Arvind Ahluwalia, MS K141
14300 Alton Parkway
Irvine, CA 92718-1814

1 SAFT America
Attn: K. K. Press
Doug Briscoe
107 Beaver Court
Cockeysville, MD 21030

1 Technochem Co.
Attn: Shyam Argade
203A Creekridge Rd.
Greensboro, NC 27406

1 DRA Haslar
Materials Dept.
Attn: A. G. Ritchie
Gosport
Room F8, AC Building
Hampshire PO 12 2AG
ENGLAND

1 Leclanche, S.A.
Attn: P. Reutschi
48, Avenue de Grandson
CH-1401 Yverdon-Les-Bain
SWITZERLAND

2 ASB
Att: A. J. Clark
Serge Schoeffert, Research Mgr.
Allée Ste Hélène
18000 BOURGES CEDEX
FRANCE

1	MS0614	P. C. Butler, 2522
1	MS0614	A. H. Andazola, 2522
1	MS0614	F. P. Lasky, 2522
1	MS0614	F. W. Reinhardt, 2522
5	MS0614	R. A. Guidotti, 2522
1	MS0614	R. W. Bickes, 2523
1	MS0614	L. M. Moya, 2523
1	MS0614	L. Demo, 2523
1	MS0614	J. A. Gilbert, 2523
1	MS1453	G. L. Scharrer, 2553
1	MS9018	Central Technical Files, 8490-2 1
2	MS0899	Technical Library, 9616
1	MS0612	Review Approval Desk, 9612 for DOE/OSTI